

Self-Testing Graph States Permitting Bounded Classical Communication

Uta Isabella Meyer, Ivan Šupić, Frédéric Grosshans, and Damian Markham
Sorbonne Université, CNRS, LIP6, F-75005 Paris, France

(Dated: April 5, 2024)

Self-testing identifies quantum states and correlations that exhibit non-locality, distinguishing them, up to local transformations, from other quantum states. Due to their strong non-locality, all graph states can be self-tested with strictly local measurement devices. Moreover, graph states display non-local correlations even when bounded classical communication on the underlying graph is permitted, a feature that has found applications in proving a circuit-depth separation between classical and quantum computing. In the framework of bounded classical communication, we show that certain graph states with appropriate symmetry can be robustly self-tested, by providing an explicit self-test for the circular graph state and the honeycomb cluster state. Since communication generally obstructs self-testing of graph states, we further provide a procedure to robustly self-test any graph state from larger ones that exhibit non-local correlations in the communication scenario. Furthermore, in the standard setup without classical communication, we demonstrate that any graph state from an underlying connected graph with at least three vertices can be robustly self-tested using only Pauli measurements.

I. INTRODUCTION

Bell nonlocality describes a phenomenon in which entangled particles display correlations that elude classical explanations [1, 2]. Such correlations are exposed in the so-called Bell scenario where two or more non-communicating parties receive some classical inputs and return classical outputs. A description of the outputs' correlations through local hidden variable models (LHV) leads to the formulation of a Bell inequality whose violation implies that the involved parties share some non-classical resources. Thus, the Bell scenario is considered a prime stage for witnessing quantumness.

The concept of certification, commonly referred to as 'device-independence', has emerged as a highly productive research avenue over the past two decades [3–8]. A simple violation of a Bell inequality witnesses the presence of entanglement in the joint state of all the parties. Although LHV models cannot reproduce all Bell nonlocal correlations, certain correlations exhibit exceptional strength and are exclusive to a specific state, up to to a well-defined set of transformations. When a quantum state is capable of generating correlations that are unattainable not only by LHV models but also by any other quantum state, we say that such a state can be self-tested [9–11]. Observing correlations that self-test some quantum state can be seen as a device-independent certificate of that state. Besides witnessing entanglement of a particular quantum state, many other quantum information protocols have been constructed as device-independent by embedding them in the Bell scenario [12–17].

A common feature among all device-independent protocols is their reliance on violations of Bell inequalities, which necessitates spatial separation and prohibits communication among the participating parties. This requirement can be alleviated by ensuring that the parties are shielded, preventing the transmission of

information regarding the Bell input, i.e., the type of measurement performed, to any other party. Fulfilling this condition poses a considerable challenge, particularly in scenarios involving the creation of multipartite states on integrated photonics platforms [18, 19].

An intriguing question arises regarding the impact of self-testing when the absence of communication among parties cannot be guaranteed. To date, this scenario has not received any attention, with a notable exception being [20]. In this work, Murta and Baccari explore the potential for self-testing Greenberger-Horn-Zeilinger (GHZ) states within scenarios featuring clusters of parties capable of broadcasting received inputs to all parties within a given cluster. Their findings are significant, revealing that even when N parties are partitioned into k separate clusters, each accommodating dishonest parties, it remains possible to self-test k -partite GHZ states. This outcome aligns with the intuition that within a Bell scenario involving N parties, any form of communication effectively diminishes the certifiable resource size. Indeed, as elucidated in [20], only a quantum resource shared among non-communicating clusters is susceptible to self-testing. Our study challenges this intuition by demonstrating that certain quantum states can be fully self-tested even in scenarios where some degree of communication is permitted among subsets of parties, regardless of whether they are disjoint — an outcome that constitutes our main result.

From a broader perspective, such a result underscores the significance of interaction, one of the most important concepts in computational complexity theory. In essence, the Bell scenario resembles a form of multipartite interactive proof, wherein a verifier engages with multiple, ideally non-communicating provers [21]. While the provers may attempt to deceive by engaging in communication amongst themselves, the verifier can also thwart dishonest behavior by providing inputs to the provers that are not factored into the certification process. In doing so, the provers' deceptive actions are

effectively countered, as they are misled into replicating a predetermined behavior. This notion of influential yet misguided interaction will be formally elucidated in the subsequent section. For the remainder of this section, we provide a high-level overview of the scope of this paper, refraining from technical details.

Our main subject of interest are graph states, which represent a multifaceted resource in quantum information processing. Being multipartite states with regular entanglement structure and compact form, they proved to be useful in a wide range of quantum technologies, from measurement-based [22] and fusion-based [23] quantum computing to topological error correction [24, 25], quantum metrology [26], and cryptography [27, 28]. The experimental realization of graph states has allowed for the demonstration of controlled genuine multipartite entanglement [29–31], and the implementation of various quantum information protocols [32, 33]. Graph states are a strong resource for Bell nonlocality, as for every entangled graph state there exist local quantum measurements leading to a violation of some Bell inequality [34, 35].

In the context of nonlocality involving communication, Barrett et al. [36] present correlations based on Pauli operators in a graph state that no LHV model, even assisted by a round of restricted classical communication, can reproduce. We call such a model d -LHV* for a communication range up to distance d along the edges of the graph. This result had application in the design of distributed computation protocols [37], randomness extraction [38], and on establishing an unconditional proof of a computational quantum advantage [39, 40]. In [41], the result of Barrett et al. [36] was extended to one based on any graph state by introducing the so-called inflated graph states. The inflated graph states then exhibit correlations that are impossible to reproduce by any d -LHV* model.

In our study, we demonstrate that graph states exhibiting a high degree of symmetry can be self-tested through correlations derived from Pauli measurements, which defy the explanation by any d -LHV* model. Leveraging techniques akin to those employed in scenarios with non-communicating devices, we present two specific experiments: one involving large circular graph states and the other focusing on the honeycomb cluster state. However, in the case of general graph states, the potential for deception by communicating devices renders the self-testing of such states unfeasible. To address this challenge, we propose a novel approach that enables the self-testing of any graph state by expanding it into an inflated graph state, permitting limited classical communication on this augmented state. By assessing correlations that surpass the capabilities of any d -LHV* model, we can confirm that subsequent local measurements on the added vertices result in a post-measurement state that is locally isometric to the original graph state. This is achieved through the introduction of three types of correlations, one of which applies to any inflated graph

state. To achieve full self-testing of the honeycomb graph and the odd circular graph while still permitting limited classical communication, we employ these same three instances without inflating or deflating the graph.

Additionally, for scenarios involving non-communicating devices, we present a self-test utilizing Pauli measurements for any graph state featuring at least three connected vertices in a line. When combined with the findings of McKague [42], this approach facilitates the verification of any graph state with at least three connected vertices using local devices capable of performing Pauli operations.

The structure of the article is as follows: We commence with an introduction to self-testing and graph states in Section II. In Section III A, we discuss the general characteristics of self-testing graph states with communication patterns determined by an underlying graph. This is followed by technical definitions in Section III B, and the introduction of three types of self-testing correlations in Section III C. Our first result is presented in Section III D, where we demonstrate the self-testing of graph states from inflated graph states, allowing for restricted communication. In Section III E, we highlight the ability to entirely self-test the graph state of certain symmetric graphs, even in the presence of restricted communication. Finally, we offer concluding discussions in Section IV.

II. SELF-TESTING AND GRAPH STATES

We consider a multipartite Bell scenario where n non-communicating parties share a quantum state $|\Psi\rangle$. Each party i receives a classical input $k_i \in \{0, 1, \dots, m-1\}$ and performs a measurement described by an observable \mathcal{A}_{k_i} . Note that throughout this work, we focus on observables with two outcomes, although our concepts can be readily extended to include more outcomes. From the outcomes of their measurements, the expectation values $\langle \Psi | \mathcal{M}_k | \Psi \rangle$ can be estimated, where $\mathcal{M}_k = \bigotimes_{i=1}^n \mathcal{A}_{k_i}$ with $k \in \{(0, 1, \dots, m-1)^n\}$. Sometimes, as highlighted in [36], it is practical to send inputs to the parties but disregard the outputs, focusing only on the marginal correlations. To facilitate this, we introduce the concept of submeasurements, as defined in [41]:

Definition 1 (Submeasurements). *Given a measurement $\mathcal{M}_k = \bigotimes_{i=1}^n \mathcal{A}_{k_i}$ with $k \in \{(0, 1, \dots, m-1)^n\}$, a valid submeasurement \mathcal{C}_k of \mathcal{M}_k is defined as a tensor product $\mathcal{C}_k = (\mathcal{M}_k)_I = \bigotimes_{i \in I} \mathcal{A}_{k_i}$ where $I \subseteq \{1, \dots, n\}$.*

Note that in the general setting with communication the subscript is extended in a natural way to indicate dependence on communicated information.

A tuple $(|\Psi\rangle, \mathcal{M}_k)$ is termed a *physical experiment* (PE). The PE remains fully uncharacterized, with all information deriving solely from the observed measurement statistics. The goal of *self-testing* is to demonstrate that, under certain circumstances, the PE can be

deemed equivalent to another perfectly characterized setup known as the *reference experiment* (RE). Given the inherent noise in real measurement devices, the self-test must be resilient to minor perturbations. Informally, a self-testing procedure exhibits robustness if it can ascertain that the PE closely resembles the RE whenever it nearly reproduces the self-testing correlations.

When establishing a relationship between a PE and a RE, the initial step is to assess their comparability. They are deemed *compatible* if they entail the same number of local devices and measurements. A crucial subsequent condition is that the PE must simulate the RE.

Definition 2 (ϵ -Simulation). *Given a physical experiment $(|\Psi\rangle, \{\mathcal{M}_k\})$ and a compatible reference experiment $(|\psi\rangle, \{M_k\})$, the physical experiment ϵ -simulates the reference experiment if, for all k ,*

$$|\langle\psi|C_k|\psi\rangle - \langle\Psi|C_k|\Psi\rangle| \leq \epsilon, \quad (1)$$

for all submeasurements $C_k(C_k)$ of $M_k(\mathcal{M}_k)$.

In principle, this definition of simulation is marginally stronger than the one utilized in [42], where only the expectation values of measurements are considered. Nonetheless, it is somewhat intuitive that, given two experiments, one would naturally expect all sub-statistics to match if they are equivalent. Meeting this condition implies that, at the simulation level, the RE becomes indistinguishable from the experiment. Intrinsically indistinguishable features, not captured by the Bell experiment, are local rotations of all measurements and the state, as well as introducing additional degrees of freedom to the reference state where the RE's measurements act trivially. The resulting transformation are encompassed by the notion of local isometry. Thus, the two experiments are considered equivalent if they are linked by a local isometry. When the simulation of the RE by the PE suggests their equivalence, we assert that the simulating correlations (1) self-test the RE.

Definition 3 (δ -Equivalence). *Let $(|\Psi\rangle, \{\mathcal{M}_k\})$ be a physical experiment, where $|\Psi\rangle$ is a pure state on the Hilbert space $\bigotimes_{i=1}^n \mathcal{H}_i$, and $\mathcal{M}_k = \bigotimes_{i=1}^n \mathcal{A}_{k_i}$, where \mathcal{A}_{k_i} are Hermitian and unitary operators on \mathcal{H}_i . Given a compatible reference experiment $(|\psi\rangle, \{M_k\})$, where $|\psi\rangle$ is a pure state on $\bigotimes_{i=1}^n \mathcal{H}'_i$ and $M_k = \bigotimes_{i=1}^n A_{k_i}$, which simulates the physical experiment. We say that the reference experiment is δ -equivalent to the physical experiment if there exist a valid quantum state $|junk\rangle$ on Hilbert space $\bigotimes_{i=1}^n \mathcal{H}''_i$ and local isometries $\{\Phi_i : \mathcal{H}_i \rightarrow \mathcal{H}'_i \otimes \mathcal{H}''_i\}_{i=1}^n$ constituting $\Phi = \bigotimes_{i=1}^n \Phi_i$, such that*

$$\|\Phi(|\Psi\rangle) - |\psi\rangle \otimes |junk\rangle\|_1 \leq \delta, \quad (2)$$

$$\|\Phi(\mathcal{A}_{k_i}|\Psi\rangle) - A_{k_i}|\psi\rangle \otimes |junk\rangle\|_1 \leq \delta, \quad \forall k_i. \quad (3)$$

Definition 4 (Robust Self-testing). *We say that the set of correlations $\{\langle\psi|C_k|\psi\rangle\}_k$ robustly self-test the reference experiment $(|\psi\rangle, \{C_k\})$ if, for every physical experiment that ϵ -simulates the reference experiment, there exists*

a function $\delta(\epsilon)$ continuous at 0 such that the reference experiment is δ -equivalent to the physical experiment.

In the following, we focus on self-testing graph states with observables corresponding to Pauli or Clifford measurements. A graph state $|G\rangle$ is uniquely defined by a mathematical undirected graph $G = (V, E)$, a set of vertices V and edges $E \subseteq V \times V$. Every vertex represents a qubit and the graph state is defined by

$$|G\rangle = \prod_{(u,v) \in E} CZ_{(u,v)}|+\rangle^{\otimes V}, \quad (4)$$

with the Pauli X eigenstate $|+\rangle = (|0\rangle + |1\rangle)/\sqrt{2}$ and the entangling gate $CZ = (|0\rangle\langle 0| \otimes \mathbb{1} + |1\rangle\langle 1| \otimes Z)$ and the Pauli Z operator. Every graph state is equally defined by an Abelian subgroup of the Pauli group, called the stabilizer group, that is generated by $g_u = X_u \otimes_{v \in N(u)} Z_v$ for every vertex u and its neighbors $N(u) = \{v : (u,v) \in E\}$. The graph state $|G\rangle$ is the simultaneous $(+1)$ -eigenstate of the entire stabilizer group, in particular $g_u|G\rangle = |G\rangle$, and any stabilizer element can be written as $S = \prod_{u \in U} g_u$ for some subset $U \subseteq V$.

The stabilizer formalism for graph states imposes restrictions on the outcome of any Pauli measurement $M = \bigotimes_{v \in V} A_v$ with local outcomes $\{a_v : v \in V\}$. In a nonlocal paradox for graph states, it is often employed that the above restrictions lead to an incompatibility with classical variables assigned to the measurement's outcomes. The chosen measurements exploit that the classical variables follow a commuting algebra, while the operators constituting the measurement anti-commute. No local hidden variable (LHV) model can describe all correlations of a graph state from a non-trivially connected graph [34, 43]. McKague has demonstrated robust self-testing of all connected graph states, characterized by robustness bounds of $\delta(\epsilon) \sim \mathcal{O}(\sqrt{\epsilon})$ or $\delta(\epsilon) \sim \mathcal{O}(\sqrt[3]{\epsilon})$ [42, 44]. Their proof implicitly use the following proposition.

Proposition 1. *For self-testing graph states, the following two conditions on the observables of the physical experiment are necessary and sufficient.*

First, the local observables (ϵ -)certify a qubit in the sense that there exist at least two binary local observables that (ϵ -)anti-commute with respect to their action on the state.

Second, the same local observables (ϵ -)reproduce the graph state's stabilizer conditions. At minimum, the set of correlations are a generating set of the stabilizer group, for instance the generator elements.

The first condition is achieved by checking nonlocal correlations of the graph state. The simulation condition of Def. 2 imposes the restrictions from the nonlocal correlations. To comply with the restrictions, the PE observables must locally anti-commute with respect to their action on the PE's state. For the second condition,

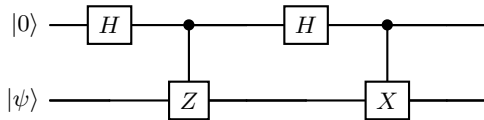


FIG. 1: The quantum circuit implements a SWAP gate between an input state $|\psi\rangle$ and the state $|0\rangle$ with the Hadamard gate H and Pauli operators X, Z .

the RE test the graph state's generator elements g_u . The observables that we show (ϵ -)anti-commutativity for reproduce the correlations of the graph's generator elements. With these properties, one constructs a local isometry that implements a SWAP gate between the PE's state and an auxiliary qubit for every vertex. The isometry was first introduced in [9] and is a product of isometries whose circuit description is in Fig. 1. The resulting state on the auxiliary qubit is proven to be (δ -)equivalent to the graph state from the RE. In Appendix A, we exemplify this approach by providing a self-test for any graph state with three connected vertices in a line with a RE that relies on correlations that constitute a Greenberger-Horn-Shimony-Zeilinger (GHSZ)-like paradox [45]. This new self-test has robustness of $\delta(\epsilon) \sim \mathcal{O}(\sqrt{\epsilon})$, with a slight improvement in scaling for some cases compared to [42, 44]. To self test all graph states, the remaining case of a pair of vertices and those where the graph consists only of triangles, are already covered in [42]. For our main results below, we use the above ideas to show that some graph states can be self-tested even if some classical communication is permitted, which lifts the devices' strict locality.

III. SELF TESTING GRAPH STATES AGAINST BOUNDED CLASSICAL COMMUNICATION

This section contains a description of the main result of this manuscript. Subsection III A describes some specificities of self-testing in the scenario allowing communication. The central concept of an inflated graph state and its inflated generator elements are introduced in Subsection III B. Every graph state can be seen as being represented by one of the three groups, which motivates our three reference experiments introduced in III C. A general method for self-testing graph states through the process of inflation and deflation is described in Subsection III D. Finally, in III E we show that some symmetric graph states can be self-tested directly, even if some amount of classical communication is allowed, which is the main surprising result of this work.

A. Conceptual features of self-testing with communication

We will now explore the extension of the ideas introduced in Section II to accommodate a single round of communication between the devices. Integrating communication into the self-testing framework primarily entails precisely defining the physical experiment (PE), particularly determining the observables associated with the measurements performed. In the conventional self-testing scenario, each observable is solely indexed by a local input, reflecting the local choice of measurement setting. This limitation stems from the premise that devices are kept unaware of activities at other locations. However, in scenarios permitting communication, the physical observables may also depend on the information (i.e., the measurement setting choices) made at locations within the communication range.

In this work, inspired by [36, 41], we adopt the notion that allowed communication is dictated by the graph state of the PE. Each device can broadcast to the devices a distance d away on the graph G defined by the associated graph state. The extension of LHV models to this communication setting is denoted as d -LHV* models. Our work uses tests that contradict any d -LHV* model based on [41], which is our main motivation for this choice of communication setting, which matches that of the original example in [36]. This setting has already found applications to prove computational [39, 40] and communication complexity [37] separations, as well as certified randomness expansion [38].

We now define the PE in the communication scenario. Consider a graph $G = (V, E)$ with local parties on the vertices that share a quantum state $|\Psi\rangle$ and are allowed to classically communicate dictated by an underlying graph up to distance d along the graph's edges. Upon receiving a classical input $k_u \in \{0, 1, \dots, m-1\}$, each party u broadcasts the classical input to all vertices in $N_d(u)$ and performs a binary measurement according to an observable $\mathcal{A}_{k_u^{(d)}}$ where $k_u^{(d)} = (k_u, (k_v)_{v \in N_d(u)})$. That is, each measurement is indexed by the local measurement choice and those of its neighbours up to distance d . The whole measurement is described by the tensor product $\mathcal{M}_k = \mathcal{A}_{k_u^{(d)}}$ and $k \in \{(0, 1, \dots, m-1)^{|V|}\}$. The experiment can also check the submeasurements $\mathcal{C}_k = (\mathcal{M}_k)_{U_k} = \bigotimes_{u \in U_k} \mathcal{A}_{k_u^{(d)}}$ for $U_k \subseteq V$. Note that the number of local measurement settings is larger than in a scenario without communication. When comparing the PE to a reference experiment (RE), we can w.l.o.g. assume that the RE's local measurement settings with inputs $k \in \{(0, 1, \dots, m-1)^{|V|}\}$ increase in the same way, even if, in practice, the observables are indifferent of the communication.

Within the framework of the above PE setting, we now leverage the definitions of simulation 2 and equivalence 3 to investigate self-testing within a communication scenario. Our objective is to achieve self-testing of

a graph state $|G\rangle$, for which we propose two distinct methods.

In the first approach, applicable to graphs exhibiting appropriate symmetry, we present an RE consisting of the graph state $|G\rangle$ and a set of local measurements. We use these correlations to self-test the reference state, even when the devices are allowed to communicate up to distance d on G . Nonetheless, this method is contingent upon certain symmetrical properties, and its applicability to all graph states cannot hold. For instance, in the case of a state corresponding to a fully connected graph, the allowed communication means that each party would possess complete information, thus enabling classical replication of all conceivable correlations by the devices.

Our second approach is universally applicable to all graph states. In this method, given a target graph state $|G\rangle$ for self-testing, the RE incorporates a larger graph state known as an inflated graph state, and a set of local measurements. The communication is defined with respect to this larger state (hence its tractability), and the local measurements serve both to prepare the target graph state $|G\rangle$, and to provide correlations which self test it. In this way, if a PE faithfully simulates this RE, the equivalence between the post-measurement (deflated) physical state and the target graph state can be established, even in scenarios permitting limited communication among the parties involved. This is illustrated for the RE in Fig. 2. Since the first approach uses ideas and techniques from the second approach, we start by presenting the second, more general approach.

B. Inflated graph states

Following [41], given a graph G , the inflated graph state G' is defined by adding d vertices along each edge. We call these added vertices *chain* vertices, and the original vertices *power* vertices. The associated *inflated graph states*, have been shown to exhibit correlations that contradict any d -LHV* model [41], and are a key tool in our approach. Formally the inflated graph is defined as follows.

Definition 5 (Inflated graph). *Given a graph $G = (V, E)$, its d -inflated graph $G' = (V', E')$ replaces all edges with a connected chain of $2d$ vertices bridging the original edge. The new vertices $V' = V \cup W$ consist of those from the original graph V , referred to as power vertices, and the new chain vertices $W = \{r_{(u,v)}; r = 1, \dots, 2d, (u,v) \in E\}$. The new edges are $(u, 1_{(u,v)}), (1_{(u,v)}, 2_{(u,v)}), \dots, ((2d)_{(u,v)}, v) \in E'$.*

Note that although the edges are symmetric $(u, v) = (v, u)$, our notation for the chain vertices is not; instead, we count r from the vertex u to the vertex v . In this regard, we can also use the terms ‘left’ and ‘right’. Given an inflated graph state $|G'\rangle$, when the chain vertices of are measured in Pauli X or Pauli Y , we get back the original graph state $|G\rangle$, up to local Pauli

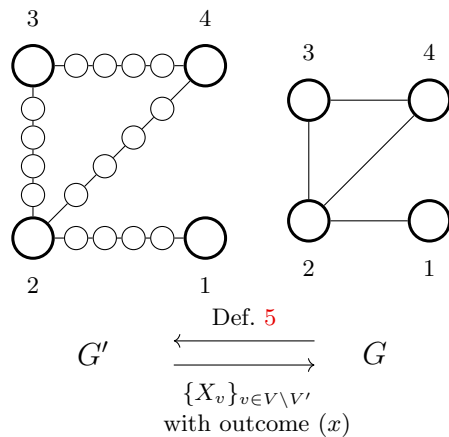


FIG. 2: A graph with four vertices (RHS) is mapped to an exemplary *inflated* graph for $d = 2$ (LHS) by means of Def. 5 by adding $2d$ vertices (called chain vertices) along the edges (Def. 5). The inverse mapping, *deflation*, takes the corresponding inflated graph state (LHS) back to the graph state (RHS) by projective measurements on the chain vertices (up to local corrections). In Theorem 1, we use this map to self-test the graph state $|G\rangle$ from the inflated graph state $|G'\rangle \rightarrow |G\rangle \sim |G^{(x)}\rangle = \bigotimes_{v \in V \setminus V'} \Pi_v^{(x)}(X_v)|G'\rangle$. That is, our reference experiments (consisting of the inflated graph states and sets of local measurements) both prepare the graph state, and self test it at the same time.

corrections (which are a function of the measurement outcomes). We call this process *deflation*. This is easy to see from the well known rules of graph transformation when measuring Pauli operators on a graph state [46]. An example of an inflated graph, and its deflation is depicted in Fig. 2. For every d -inflated graph state, there exist Pauli measurements that generate correlations inconsistent with any d -LHV* models [41]. For a graph with at least three connected vertices, this inconsistency is demonstrated by means of a GHSZ-like paradox [45]. In the case of a graph comprising two connected vertices, the incompatibility is established via an inequality akin to the Clauser-Horne-Shimony-Holt (CHSH) inequality [47].

Finally, it will be useful later to define the so called *inflated generator element*, which emulates the generator element of the original graph on the power vertices of the inflated graph. Denoting the generator elements of the inflated graph states as $\{g'_u\}_{u \in V'}$, we define it as follows.

Definition 6 (Inflated Generator Element). *The inflated generator element f_u is a stabilizer element of the inflated graph state with*

$$f_u = g'_u \prod_{\substack{(u,v) \in E, \\ s=1, \dots, d}} g'_{2s_{(u,v)}}. \quad (5)$$

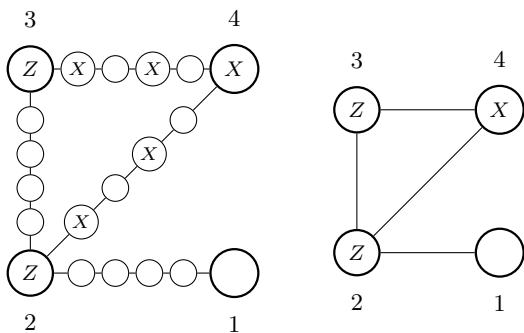


FIG. 3: A graph with four vertices (RHS) is mapped to an exemplary inflated graph for $d = 2$ (LHS) by means of Def. 5. The letters inside the nodes indicate the non-trivial Pauli operator while empty nodes indicate Pauli identity in the Pauli product of the inflated generator element f_4 from Def. 6 (LHS), mimicking the generator element g_4 (RHS) on the corresponding graph state.

An example of an inflated generator element is illustrated in Fig. 3. The inflated generator elements, and the deflation measurements will appear, amongst others, in the reference experiments that will allow us to simultaneously prepare the target graph state (through deflation) and self test it (coming from the fact that the correlations contradict any d -LHV* model [41]).

C. Reference experiments

We introduce three REs that comprehensively address any inflated graph state. Each RE comprises the inflated graph state, measurements containing submeasurements corresponding to every inflated generator element, and a set of measurements from which we can find submeasurements whose outcomes challenge any d -LHV* model. For clarity and simplicity, we opt to present the submeasurements alongside the measurements they originate from.

In order to show self testing, the reasoning follows proposition 1, first by showing anti-commutation in the measurements. The correlations observed in the submeasurements, which challenge any d -LHV* model, demonstrate an anticommutation relation between two observables on at least one power vertex. Utilizing this relation, we can derive an anticommutation relation for two observables on any other connected power vertex, leveraging the submeasurements corresponding to the inflated stabilizer elements. Subsequently, we construct an isometry using these observables, which maps the given state to the graph state. Note that this process holds true for any degree of inflation d . Before introducing our REs, let us define the concept of an induced subgraph:

Definition 7 (Induced subgraph). *An induced subgraph*

of a graph $G = (V, E)$ is a subset of vertices $U \subset V$ along with the edges $(U \times U) \cap E$ of the original graph if and only if the edge connects two vertices in the subset U .

The first RE is applicable when the corresponding graph contains an odd circle as an induced subgraph, and in particular a triangle subgraph. The second RE is suitable for graphs with an induced star subgraph, i.e., a central vertex whose nearest neighbors do not share an edge. These two cases encompass any graph with at least three vertices. The third RE is applicable to graphs with a pair of neighboring vertices, i.e., any connected graph and specifically the graph comprising only two connected vertices. Note that, in fact, any connected graph can be covered by the third RE, in this sense we do not need the first or second REs, but they are nevertheless useful to have since they can be more robust. Indeed the different REs can be in principle combined in different ways to optimise robustness for example. Robustness is treated in appendix F

For all three REs, the local measurements on the chain vertices, which deflate the inflated graph state as described in Eq. (11) of Theorem 1, correspond to measurements in the Pauli X basis, as depicted in Fig. 2. The only exception occurs in RE 3 when the original graph consists solely of a pair of vertices. In this scenario, the two nearest neighbors of vertex v_m measure in the Pauli Y basis. However, both RE 2 and RE 3 incorporate measurements where certain chain vertices also measure in the Pauli Y basis. We present the submeasurements C in terms of the stabilizer elements of the graph state. Their corresponding representations as Pauli tensor products are in the Appendix B. Recall that g'_u for $u \in V'$ denotes a generator element of the inflated graph state, f_v denotes an inflated generator element from Eq. (5) and, for a subset of vertices U , we define

$$h_U^U = \prod_{\substack{v \in N(u) \setminus U, \\ s=1, \dots, d}} g'_{2s(u,v)}.$$

Reference Experiment 1 (Odd Circular Subgraph). *Let G' denote the inflated graph derived from a connected graph $G = (V, E)$ containing a circular subgraph $G_c = (V_c, E_c)$ with an odd number of vertices, and let $|G'\rangle$ denote the corresponding inflated graph state $|G'\rangle$.*

We consider the operators f_u from Eq. (5),

$$C_V = (-1) \prod_{v \in V_c} f_v, \quad (6)$$

$$C_u = h_u^{V_c} \prod_{v \in V_c \setminus \{u\}} f_v, \quad (7)$$

and $Z_u C_u$ for all $u \in V_c$.

The reference experiment consists of the state $|G'\rangle$ and the Pauli measurements M defined by the above Pauli tensor product with Pauli X operators applied wherever the Pauli tensor product involve identity operators.

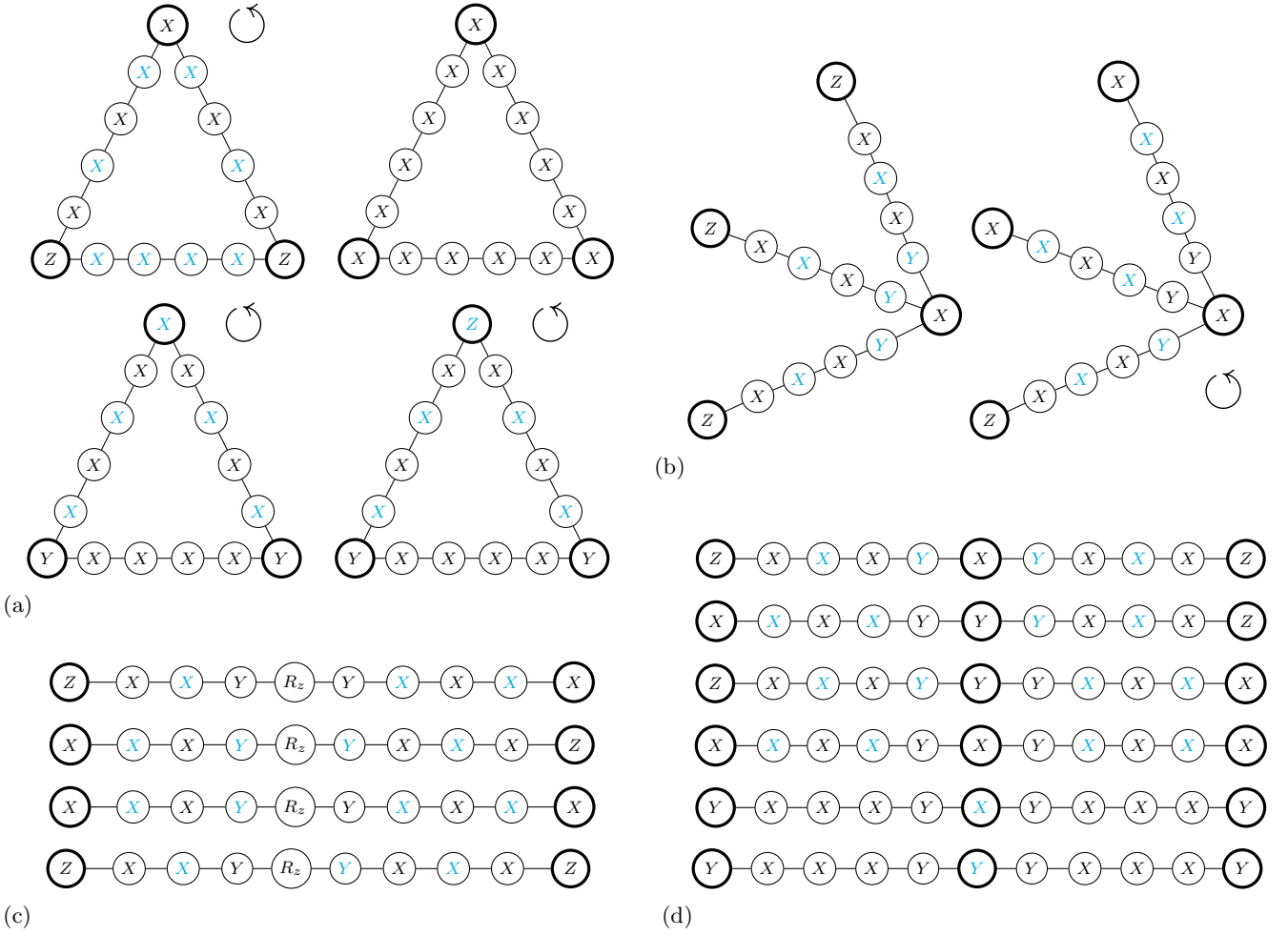


FIG. 4: We illustrate four inflated graphs with the highlighted power vertices that exemplify the induced subgraphs used in the reference experiments 1, 2, and 3. The letters in black and light-blue font indicate the Pauli operators on the vertices in the tensor product corresponding to the local Pauli measurement. For the submeasurements, the letters in light-blue font are not considered but have Pauli identity in their tensor product representation. Graphs with a circular arrow represent all measurements under invariant rotations of the power vertices. (a) The four graphs illustrate the submeasurements f_u (upper left) from Eq. (5) (Eq. (B1)), C_V (upper right) from Eq. (6) (Eq. (B5)), and twice C_u (lower) from Eq. (7) (Eq. (B6)). (b) The left graph illustrates the submeasurements from the inflated generator element f_{v_c} from Eq. (5) (Eq. (B1)) of the central vertex v_c of the star graph. The right graph illustrates the submeasurements C_{v_i, v_j} from Eq. (8) (Eq. (B11)). (c) The four graphs illustrate the submeasurements I_1, I_2, I_3, I_4 from Eq. (10) and Eqs. (B22)-(B25) (top to bottom). For an illustration of P_1, P_2 in Eq. (B26) and Eq. (B27) replace R_z by X in the first two graphs. (d) The six graphs illustrate the submeasurements, from top to bottom, f_{v_c} in Eq. (5) (Eq. (B1)), for the central vertex v_c , $C_{v_1}, C_{v_2}, C_{v_c}$ and twice C_2 from Eq. (9), (Eqs. (B11)-(B16)).

The Pauli tensor products f_u , C_V , and C_u in RE 1 are proportional to stabilizer elements of the inflated graph state and considered as submeasurements of the Pauli measurements. Their representations with Pauli operators are provided in Appendix B, and illustrated in Fig. 4a.

Reference Experiment 2 (Star Subgraph). Let G' denote the inflated graph derived from a connected graph $G = (V, E)$ that contains an induced star subgraph, i.e., a vertex v_c with at least two adjacent vertices that do not

share an edge. Let $|G'\rangle$ denote the corresponding inflated graph state.

If $|N(v_c)| > 2$, we select a set $V_3 = \{v_1, v_2, v_3\} \subseteq N(v_c)$, and, for $v_i, v_j \in V_3$ and $v_i \neq v_j$, we consider the operators f_{v_c} from Eq. (5), and

$$C_{v_i v_j} = (-1) g'_{v_c} f_{v_i} f_{v_j} h_v^{\{v_i, v_j\}}. \quad (8)$$

If $N(v_c) = \{v_1, v_2\}$, particularly when $|N(v_c)| = 2$, we

consider

$$\begin{aligned} C_{v_1} &= g'_{v_c} f_{v_1} h_{v_c}^{\{v_1\}}, & C_{v_2} &= g'_{v_c} h_{v_1}^{\{v_2\}} f_{v_2}, \\ C_{v_c} &= -g'_{v_c} f_{v_1} f_{v_2}, & C_2 &= f_{v_1} f_{v_2} h_{v_c}, \end{aligned} \quad (9)$$

and $Y_{v_c} C_2$.

The reference experiment consists of the state $|G'\rangle$, and several sets of measurements. First, the Pauli measurements defined by the above tensor product operators with Pauli X operators applied wherever the Pauli tensor product involve identity operators, except for the nearest neighbors of v_c that measure in the Pauli Y basis. Second, the reference experiment also contains the Pauli measurements defined by f_u for all $u \in V$ with Pauli X operators wherever the tensor product operators involve identity operators.

The tensor product operators f_u , C_{v_i, v_j} , and $C_{v_1}, C_{v_2}, C_{v_c}, C_2$ in RE 2 are proportional to stabilizer elements of the inflated graph state and considered as submeasurements of the Pauli measurements. Their representations with Pauli operators are provided in Appendix B, and illustrated in Figs. 4b and 4d.

Reference Experiment 3 (Vertex Pair). Let G' denote the d -inflated graph derived from a connected graph $G = (V, E)$ with two neighboring vertices v_l and v_r , and $|G'\rangle$ denote the corresponding inflated graph state.

We consider the operators f_u from Eq. (5) for all $u \in V \setminus \{v_l, v_r\}$, and

$$\begin{aligned} P_1 &= (-g'_{v_m})^{d+1} f_{v_r}, & P_3 &= (g'_{v_m})^d \tilde{f}_{v_l}^{(e)} \tilde{f}_{v_r}^{(e)} \\ P_2 &= (-g'_{v_m})^d f_{v_l}, & P_4 &= (g'_{v_m})^{d+1} \tilde{f}_{v_l}^{(o)} \tilde{f}_{v_r}^{(o)}. \end{aligned}$$

where $v_m := d_{(v_l, v_r)}$, and with

$$\tilde{f}_{v_a}^{(e)} = h_{v_a}^{\{v_b\}} \prod_{s=1}^{\lfloor d/2 \rfloor} g'_{2s(v_a, v_b)}, \quad \tilde{f}_{v_a}^{(o)} = h_{v_a}^{\{v_b\}} \prod_{s=1}^{\lfloor d/2 \rfloor} g'_{(2s-1)(v_a, v_b)},$$

for $a, b \in \{l, r\}$. Moreover, we consider the tensor product operators

$$I_i = \frac{1}{\sqrt{2}} \left(P_i + \sqrt{Z}_{v_m} P_i \sqrt{Z}_{v_m}^\dagger \right), \quad (10)$$

for $i = 1, 2, 3, 4$, with the phase gate \sqrt{Z} applied on vertex v_m .

The reference experiment consists of the state $|G'\rangle$ and the Pauli measurements defined by the above Pauli tensor products with Pauli X operators applied wherever the Pauli tensor product involve identity operators, except for the nearest neighbors of v_m that measure in the Pauli Y basis.

The tensor product operators f_u, P_1, P_2, P_3, P_4 in RE 2 are proportional to stabilizer elements of the inflated graph state and considered as submeasurements of the Pauli measurements. Their representations with Pauli and Clifford operators are provided in Appendix B, and illustrated in Fig. 4c.

D. Self-testing graph states through inflation and deflation

We are now ready to state our self-testing of graph states using these three reference experiments. The idea is that given a target graph state $|G\rangle$, the REs use the inflated graph state $|G'\rangle$ to both prepare the target graph state, through deflation (whose measurements are included in the RE) and self test it (since the correlations contradict d -LHV* models, allowing to prove anti-correlation of the local observables). That is, if the PE simulates the RE for the inflated graph state, then the deflated PE is equivalent to the deflated RE which is locally equivalent to the target graph state. Formally, this is described in the following theorem.

Theorem 1. For any d -inflated graph G' derived from a connected graph G , there exists a choice of reference experiment implying the following, even when one-way classical communication is permitted up to distance d along the edges of the d -inflated graph: Given a physical experiment $(|\Psi'\rangle, \{\mathcal{M}_k\})$ that ϵ -simulates (Def. 2) the reference experiment $(|G'\rangle, \{\mathcal{M}_k\})$, then, the deflated physical experiment $(|\Psi^{(x)}\rangle, \{\mathcal{M}_k\})$ is δ -equivalent (Def. 3) to the deflated reference experiment $(|G^{(x)}\rangle, \{\mathcal{M}_k\})$ for all outcomes (x) . The deflated experiment is obtained by performing projective measurements on the chain vertices,

$$|G^{(x)}\rangle = \bigotimes_{v \in V' \setminus V} \Pi_v^{(x)}(\mathcal{M}_{k_v}) |G'\rangle, \quad (11)$$

$$|\Psi^{(x)}\rangle = \bigotimes_{v \in V' \setminus V} \Pi_v^{(x)}(\mathcal{M}_{k_v}) |\Psi'\rangle. \quad (12)$$

Here $\Pi^{(x)}(A)$ represents the product of local measurement projectors corresponding to the observables A with outcome (x) .

The measurements $M_{k_v}(\mathcal{M}_{k_v})$ in Eqs. (11) and (12) effectively implement, and then correspond to, a measurement in the Pauli X basis, which reduces the inflated graph state to the original up to local corrections as illustrated in Fig. 2.

Consider a PE with state $|\Psi\rangle$ and measurements \mathcal{M}_k with corresponding submeasurements \mathcal{C}_k that are compatible with a RE 1, 2 or 3. We distinguish measurement observables based on the local measurement setting. Specifically, we employ calligraphic font to denote measurements and observables associated with the PE, as opposed to italic font utilized for the REs. Theorem 1 is a statement on the PE's state $|\Psi'\rangle$ after measuring the chain vertices in the measurement bases corresponding to observable \mathcal{X} with outcome $\mathbf{x} = (x_v)_{v \in V' \setminus V}$,

$$|\Psi'\rangle = \Pi_{\mathcal{X}}^{(\mathbf{x})} |\Psi\rangle = \bigotimes_{v \in V' \setminus V} (\mathbb{1}_v + (-1)^{x_v} \mathcal{X}_v) |\Psi\rangle. \quad (13)$$

To establish the existence of an isometry mapping $|\Psi'\rangle$ to the graph state $|G\rangle$, the PE must satisfy the two

conditions from Proposition 1. Specifically, for every power vertex u , there exist a pair of anticommuting observables \mathcal{X}_u and \mathcal{Z}_u . Furthermore, the observables should adhere to the stabilizing conditions corresponding to the graph state $|G\rangle$, up to local corrections with $(x_e)_u := \sum_{s=1}^d x_{2s(u, N(u))}$,

$$\mathcal{X}_u \bigotimes_{v \in N(u)} \mathcal{Z}_v |\Psi'\rangle = (-1)^{(x_e)_u} |\Psi'\rangle. \quad (14)$$

An example illustrating how these two conditions, in the case of non-inflated graph states, culminate in the self-testing statement, is provided in Appendix A. This methodology has been utilized to self-test graph states in other relevant articles on the topic, as referenced in [42, 48, 49]. In our framework, the anticommutation condition is established by exploiting all the implications from the conditions that a PE is *compatible* and ϵ -*simulates* one of the RE 1, 2 or 3, which we state in the following lemma.

Lemma 1. *If a physical experiment $(|\Psi\rangle, \{\mathcal{M}_k\}_k)$ is compatible with one of the reference experiments 1, 2, or 3, and simulates it according to Def. (2) for $\epsilon = 0$, then $\{\mathcal{X}_u, \mathcal{Z}_u\}|\Psi\rangle = 0$ for all power vertices u but vertex v_l in RE 3 where $\{\mathcal{X}_{v_l}, \mathcal{X}_{v_m}^{(X)}, \mathcal{Z}_{v_l}, \mathcal{X}_{v_m}^{(Z)}\}|\Psi\rangle = 0$ for $v_m = d(v_l, v_r)$.*

The complete proof of Lemma 1 is provided in Appendix C. Conceptually, the simulation condition imposes constraints on the PE's observables, which are related to the stabilizer formalism. Additionally, certain measurement settings correspond to measurements that lead to a non-local paradox for the inflated graph state. The constraints imposed on the observables by these settings lead to an anticommutation relation for two observables on a single power vertex. From a single anticommutation relation, Lemma 2 in Appendix C extends the anticommutation relation to a neighboring power vertex. This process, applied iteratively, yields an anti-

commutation relation for every power vertex within the connected graph.

For example, consider RE 2 involving a star with a central vertex v_c , $|N(v_c)| > 2$ and a subset $V_3 = \{v_1, v_2, v_3\} \subseteq N(v_c)$ as in Fig. 4b. Note that Fig. 4b does not involve the measurements corresponding to the inflated stabilizer elements f_v , in which all chain vertices in d -neighbourhood of v_c ‘measure’ X instead of Y . We denote the PE's measurement settings simulating the submeasurements $f_v, C_{v_i v_j}$ as $\zeta_{v_i}, C_{v_i v_j}$, respectively. We distinguish the submeasurements ζ_{v_c} from $\tilde{\zeta}_{v_c}$. The submeasurement ζ_{v_c} arises from measurement configurations where all vertices within the communication range of v_c measure in the basis associated with the Pauli X operator. Conversely, for $\tilde{\zeta}_{v_c}$, the nearest neighbor vertices of v_c perform a measurement associated with the Pauli Y operator. Similarly, the observable \mathcal{X}_u is enacted when vertex u and all vertices within its communication range receive inputs corresponding to Pauli X , whereas \tilde{X}_u denotes the analogous scenario where at least one vertex within the communication range receives an input corresponding to Pauli Y . The perfect simulation conditions then imply $\langle \Psi | \tilde{\zeta}_{v_c} | \Psi \rangle = \langle \Psi | \zeta_{v_i} | \Psi \rangle = -\langle \Psi | C_{v_i v_j} | \Psi \rangle$ for $v_i \in V$. For a $v_1 \in V_3$, it thus holds

$$\tilde{\zeta}_{v_c} C_{v_1 v_2} C_{v_2 v_3} C_{v_1 v_3} |\Psi\rangle = (-1) |\Psi\rangle, \quad (15)$$

which is equivalent to the anticommutation relation $(-1)\mathcal{X}_{v_1} \mathcal{Z}_{v_1} |\Psi\rangle = \mathcal{Z}_{v_1} \mathcal{X}_{v_1} |\Psi\rangle$. The full evaluation is provided in Appendix C. Note that the observables on vertex v_1 take into account that all vertices within communication range perform measurement according to Pauli X operators. To obtain the same anticommutation relation on the vertex v_c , we evaluate $\tilde{\zeta}_{v_c} \zeta_{v_c} \tilde{\zeta}_{v_c} \zeta_{v_c} |\Psi\rangle = (-1) |\Psi\rangle$. The anticommutation relation for all other vertices follows from Lemma 2.

A simple visualization of the calculation for $d = 2$ can be depicted as an array, where each row contains the measurements \mathcal{M} with submeasurements \mathcal{C} , along with the deterministic outcome $\chi = \pm 1$ from $\mathcal{C}|\Psi\rangle = \chi|\Psi\rangle$:

$\mathcal{C}(\mathcal{M})$	χ	v_c	$1_{(v_c, v_1)}$	$2_{(v_c, v_1)}$	$3_{(v_c, v_1)}$	$4_{(v_c, v_1)}$	v_1	$1_{(v_c, v_2)}$	$2_{(v_c, v_2)}$	$3_{(v_c, v_2)}$	$4_{(v_c, v_2)}$	v_2	$1_{(v_c, v_3)}$	$2_{(v_c, v_3)}$	$3_{(v_c, v_3)}$	$4_{(v_c, v_3)}$	v_3
$\tilde{\zeta}_{v_c}$	1	\tilde{X}	$Y^{(X)}$	$\tilde{X}^{(X)}$	$\tilde{X}^{(Z)}$	$\tilde{X}^{(Z)}$	Z	$Y^{(X)}$	$\tilde{X}^{(X)}$	$\tilde{X}^{(Z)}$	$\tilde{X}^{(Z)}$	Z	$Y^{(X)}$	$\tilde{X}^{(X)}$	$\tilde{X}^{(Z)}$	$\tilde{X}^{(Z)}$	Z
C_{v_1, v_2}	-1	\tilde{X}	$Y^{(X)}$	$\tilde{X}^{(X)}$	$\tilde{X}^{(X)}$	$\tilde{X}^{(X)}$	X	$Y^{(X)}$	$\tilde{X}^{(X)}$	$\tilde{X}^{(X)}$	$\tilde{X}^{(X)}$	X	$Y^{(X)}$	$\tilde{X}^{(X)}$	$\tilde{X}^{(Z)}$	$\tilde{X}^{(Z)}$	Z
C_{v_2, v_3}	-1	\tilde{X}	$Y^{(X)}$	$\tilde{X}^{(X)}$	$\tilde{X}^{(Z)}$	$\tilde{X}^{(Z)}$	Z	$Y^{(X)}$	$\tilde{X}^{(X)}$	$\tilde{X}^{(X)}$	$\tilde{X}^{(X)}$	X	$Y^{(X)}$	$\tilde{X}^{(X)}$	$\tilde{X}^{(X)}$	$\tilde{X}^{(X)}$	X
C_{v_1, v_3}	-1	\tilde{X}	$Y^{(X)}$	$\tilde{X}^{(X)}$	$\tilde{X}^{(X)}$	$\tilde{X}^{(X)}$	X	$Y^{(X)}$	$\tilde{X}^{(X)}$	$\tilde{X}^{(Z)}$	$\tilde{X}^{(Z)}$	Z	$Y^{(X)}$	$\tilde{X}^{(X)}$	$\tilde{X}^{(X)}$	$\tilde{X}^{(X)}$	X
ζ_{v_c}	1	X	$X^{(X)}$	$X^{(X)}$	$X^{(Z)}$	$X^{(Z)}$	Z	$X^{(X)}$	$X^{(X)}$	$X^{(Z)}$	$X^{(Z)}$	Z	$X^{(X)}$	$X^{(X)}$	$X^{(Z)}$	$X^{(Z)}$	Z
ζ_{v_1}	1	Z	$X^{(X)}$	$X^{(X)}$	$X^{(X)}$	$X^{(X)}$	X	$X^{(Z)}$	$X^{(Z)}$	$X^{(X)}$	$X^{(X)}$	X	$X^{(Z)}$	$X^{(Z)}$	$X^{(X)}$	$X^{(X)}$	X
ζ_{v_c}	1	X	$X^{(X)}$	$X^{(X)}$	$X^{(Z)}$	$X^{(Z)}$	Z	$X^{(X)}$	$X^{(X)}$	$X^{(Z)}$	$X^{(Z)}$	Z	$X^{(X)}$	$X^{(X)}$	$X^{(Z)}$	$X^{(Z)}$	Z
ζ_{v_1}	1	Z	$X^{(X)}$	$X^{(X)}$	$X^{(X)}$	$X^{(X)}$	X	$X^{(Z)}$	$X^{(Z)}$	$X^{(X)}$	$X^{(X)}$	X	$X^{(Z)}$	$X^{(Z)}$	$X^{(X)}$	$X^{(X)}$	X

The Pauli measurements are represented as products of all observables shown (in black and light-blue font), while the stabilizer submeasurements consist of the products of

the observables in black font. Multiplying these column-wise yields their action on the state. The observables in the light-blue font are not directly involved in the

calculation of the anticommutation in Eq. (15), but they impact the observable within communication distance and confound classical models based on communication. All measurement observables are labeled according to the local measurement setting. The information gained from classical communication is accounted for in superscripts. To keep these minimal, we only label the chain vertices according to the measurement setting of its nearest power vertex since all other chain vertices measure in the same basis.

We now turn to the second condition for self-testing as described in proposition 1. The simulation for all four reference experiments ensures $\langle \Psi | \zeta_u | \Psi \rangle = 1$ and thus

$$\zeta_u | \Psi \rangle = | \Psi \rangle, \quad (16)$$

for the PE's observables ζ_u according to the Pauli sub-measurements corresponding to the inflated stabilizer elements f_u for all $u \in V$, and the PE's state $| \Psi \rangle$. These conditions ensure the replication of stabilizing conditions for the non-inflated graph states. However, except for the anticommuting observables \mathcal{X}_u and \mathcal{Z}_u for every power vertex, they involve \mathcal{X} (and, in some cases, \mathcal{Y}) observables on the chain vertices. After the measurement, these observables can be absorbed in the projectors

$$\Pi_{\mathcal{X}}^{(x)} \mathcal{X}_v = (-1)^{x_v} \Pi_{\mathcal{X}}^{(x)},$$

for $v \in V' \setminus V$ and traded for a sign factor. The collection of these factors turns out to be $(x_e)_u := \sum_{s=1}^d x_{2s(u, N(u))}$ from Eq. (14).

We construct an isometry as a product of the local isometries that are described by the circuit in Fig. 1. This is the standard isometry inspired by the SWAP gate and used in Appendix A and in [10, 42]. The isometry acts locally on the post-measurement state and one ancilla qubit for every power vertex.

To show the equivalence from Eq. (2) for $\delta = 0$, the post-measurement state $| \Psi' \rangle$ and the state $| G^{(\mathbf{x})} \rangle$, we follow the same procedure as in Appendix A, and the full evaluation of the isometry can be found in Appendix E. Here, we provide the final result stating that the isometry applied to the postmeasurement state (13) is

$$| G^{(\mathbf{x})} \rangle \otimes | junk \rangle = Z^{\mathbf{x}_e} | G \rangle \otimes | junk \rangle, \quad (17)$$

with the residual state $| junk \rangle = \Pi_{\mathcal{X}}^{(\mathbf{x})} \otimes_{u \in V} (\mathbb{1}_u + \mathcal{Z}_u) / \sqrt{2} | \Psi \rangle$ and $Z^{\mathbf{x}_e} = \otimes_{u \in V} Z_u^{(x_e)_u}$. Note that, for any power vertex $u \in V$, we have

$$g_u \Pi_{\mathcal{X}}^{(\mathbf{x})} | G' \rangle = g_u \Pi_{\mathcal{X}}^{(\mathbf{x})} f_u | G' \rangle = (-1)^{(x_e)_u} \Pi_{\mathcal{X}}^{(\mathbf{x})} | G' \rangle, \quad (18)$$

so that $\Pi_{\mathcal{X}}^{(\mathbf{x})} | G' \rangle$ is the eigenstate to the generator elements $(-1)^{(x_e)_u} g_u$ which implies that $| G^{(\mathbf{x})} \rangle = \Pi_{\mathcal{X}}^{(\mathbf{x})} | G' \rangle$. Regarding RE 3, note that, if the original graph is just a vertex pair, the two nearest neighbors of the vertex v_m measure in the Pauli Y basis, and the anticommutation relation on the vertex v_l depends on

observables on the chain vertices. As a result, if d is odd, the phase $(x_e)_{v_l} \rightarrow (x_e)_{v_l} + x_{v_m}$ on the vertex v_l depends in addition on the measurement outcomes of the chain vertex v_m . Moreover, if $d = 1$, we replace the observable \mathcal{X}_{v_l} by \mathcal{Y}_{v_l} in the isomorphism.

In Appendix F, we extend the proof to robust equivalence by trailing the proof for the ideal case and bounding all expressions with the techniques present in [42] and [50]. The bounds on the isometry for all the REs discussed are in Tab. I. They scale with $\sqrt{\epsilon}$ where ϵ , in Def. 4 is the deviation of the measurement results from the ideal ones. The bounds on the self-testing procedure with inflated graph states allowing bounded classical communication are slightly worse than for the non-inflated graph states, which is mainly due to the higher number of measurements required to derive the anticommutation relations.

E. Self-testing families of graph states directly

Self-testing graph states directly, while allowing for bounded classical communication dictated by the underlying graph, is, in general, impossible. Especially if the extent of the graph is small compared to the communication range, it is impossible to find constraints on the observables since the number of observables can vastly outnumber all possible measurement outcomes. We show, however, that it is possible to self-test certain graph states directly, that is, without additionally inflating or deflating them, even allowing for bounded classical communication.

We introduce two reference experiments (REs) designed for the d -inflated odd circular graph and the honeycomb cluster. It is useful to define the Pauli tensor products on a graph state

$$P_u^{(\sigma)} = \sigma_u \bigotimes_{v \in N_d(u)} X_v, \quad (19)$$

for a vertex u , its neighborhood with radius $d \geq 0$, and the Pauli operator X , all other operators are identity. Additionally, two Pauli tensor products on a graph with alternating Pauli X and Pauli Z operators are

$$\tilde{P}_u^{(X)} = X_u \bigotimes_{\substack{v \in N_d(u) \\ |u-v| \bmod 2 = 0}} X_v \bigotimes_{\substack{v \in N_d(u) \\ |u-v| \bmod 2 = 1}} X_v, \quad (20)$$

$$\tilde{P}_u^{(Z)} = Z_u \bigotimes_{\substack{v \in N_d(u) \\ |u-v| \bmod 2 = 0}} X_v \bigotimes_{\substack{v \in N_d(u) \\ |u-v| \bmod 2 = 1}} Z_v, \quad (21)$$

with $|u - v| = \text{dist}(u, v)$. The vertices in the d -neighborhood $N_d(u)$ of vertex u either have Pauli X operator, or Pauli X and Z operators in an alternating pattern.

Reference Experiment 4. Consider an odd circular graph $G = (V, E)$ and with $6d + 3$ vertices. The reference experiment consists of the graph state $|G\rangle$, and $2d + 1$ -times the measurements of RE 1 such that for an arbitrary $u \in V$, u and every $v \in N_d(u)$ serve once as a power vertex in RE 1. Furthermore, the reference experiment contains the Pauli measurements

$$\tilde{M}_u^{(X)} = \tilde{P}_u^{(X)} \prod_{v \in N(u)} P_v^{(Z)}, \quad (22)$$

$$\tilde{M}_u^{(Z)} = P_u^{(X)} \prod_{v \in N(u)} \tilde{P}_v^{(Z)}, \quad (23)$$

$$M_u^{(alt)} = \tilde{P}_u^{(X)} \prod_{v \in N(u)} \tilde{P}_v^{(Z)}, \quad (24)$$

for all $u \in V$.

Note that we are interested in the inflated generator element f_u as submeasurements of $\tilde{M}_u^{(X)}$ and $M_u^{(Z)}$, and we consider the generator element of the inflated graph state g'_u as submeasurement of the measurement $M_u^{(alt)}$.

Reference Experiment 5. Consider a honeycomb lattice $H = (V, E)$, which is a combination of two hexagonal lattices and we divide the set of all vertices accordingly into two distinct subsets V_{hex1}, V_{hex2} .

The RE consists of the honeycomb cluster state $|H\rangle$ and the measurements

$$M_1^{(alt)} = \bigotimes_{u \in V_{hex1}} X_u \bigotimes_{v \in V_{hex2}} Z_u, \quad (25)$$

$$M_2^{(alt)} = \bigotimes_{u \in V_{hex1}} Z_u \bigotimes_{v \in V_{hex2}} X_u. \quad (26)$$

Furthermore, it contains the measurements of RE 2 ($|N(v_c)| = 3$) for the d -inflated star graph on a tripoint star depicted in Fig. 5 around for an arbitrary vertex v_c . To embed the star graph and measurements from RE 2 into the honeycomb cluster, vertices adjacent to the star measure in the Pauli Z basis whenever a neighbouring vertex on the star measures in the Pauli X basis. Additionally, the reference experiment contains the Pauli measurements $\tilde{M}_{v_0}^{(X)}$ in Eq. (22) and $\tilde{M}_{v_0}^{(Z)}$ in Eq. (23) for an arbitrary vertex $v_0 \in N'(v_c)$ that is at distance $2d + 1$ from v_c on the tripoint star.

Note that we are interested in the generator elements g_v and the inflated generator elements f_v on the tripoint star for $v \in V_{hex1}$ and $v \in V_{hex2}$ respectively as Pauli submeasurements. We also consider the inflated generator elements f_{v_0}, f_{v_c} as a submeasurement of the Pauli tensor products in Eq. (22) and Eq. (23).

Theorem 2. The set of measurement correlations from the reference experiments 4 and 5, robustly self-test them respectively in terms of Def. 4, even if one-way classical communication is permitted up to distance d on the edges of the graph G given in the reference experiment.

The detailed proof of the theorem is provided in Appendix D; here, we offer an intuitive overview of the proof process.

Consider RE 4, if a physical experiment (PE) simulates $2d + 1$ times the RE 1, with each vertex alternatively serving as a power vertex or a chain vertex, Lemma 1 implies the existence of measurement observables \mathcal{X}_u and \mathcal{Z}_u for every vertex u in the inflated graph such that $\{\mathcal{X}_u, \mathcal{Z}_u\}|\Psi\rangle = 0$. This establishes the initial condition for self-testing the full graph state, which has to be complemented by the requirement that operators \mathcal{X}_u and \mathcal{Z}_v , where $v \in N(u)$, replicate the stabilizing conditions. The stabilizing correlations cannot be directly verified through reproducing $2d + 1$ times the correlations from RE 1 due to the absence of stabilizers in the form $X_u \bigotimes_{v \in N(u)} Z_v$ therein. Therefore, we incorporate submeasurements from Eq. (24). However, since communication is involved, the inputs corresponding to these submeasurements allow vertex u to measure observables different from those employed to reproduce correlations from RE 1.

Let X_u denote the local observable measured in the PE by vertex u when obtaining inputs corresponding to the Pauli tensor product (20), and Z_u for submeasurement (21). In particular, all vertices within communication distance measure in an alternating pattern according to Pauli operator X or Z . Recall that, in contrast, the local observables \mathcal{X}_u and \mathcal{Z}_u stem from measurement inputs that correspond to the Pauli tensor product (19). In particular, all vertices within communication distance measure according to Pauli operator X .

Recall that the Pauli submeasurement given in Eq. (6), in the RE 1 corresponds to the measurement having X wherever the Pauli submeasurements have identity operators. Consider now one of submeasurements from (6) in which vertex u measures X , and all vertices in its d -neighbourhood such that $|u - v| \bmod 2 = 1$ ‘measure’ identity. If we exchange the corresponding Pauli measurement in such a way that it has Z wherever the submeasurement has identity in the d -neighbourhood of vertex u , then the vertex u perceives the inputs akin to (21), leading it to measure X_u in the corresponding PE. In a similar way, in one of submeasurements from (6), in which vertex u measures according to Pauli operator Z and all vertices from its d -neighbourhood with $|u - v| \bmod 2 = 0$ ‘measure’ identity, we can exchange the corresponding Pauli measurement in such a way that it has Pauli operator Z wherever the submeasurement has identity in the d -neighbourhood of vertex u . In this case vertex, u perceives the questions corresponding to the submeasurement (20), and hence, in the PE, it will measure Z_u . Thus, from the anticommutation relation for \mathcal{X}_v and \mathcal{Z}_v , one can infer that the observables X_u and Z_u anticommute,

$$\{X_u, Z_u\}|\Psi\rangle = 0, \quad (27)$$

for $u \in V'$ in the same way it is done in proving Lemma 2.

Consequently, we acquire two pairs of anticommuting observables per vertex, denoted as $(\mathcal{X}_u, \mathcal{Z}_u)$ and (X_u, Z_u) . Notably, unlike the former pair, the latter proves instrumental in verifying the adherence to the stabilizer relations of the inflated graph state. For that, the reference experiment has to involve submeasurement consisting of $X_u \otimes_{v \in N(u)} Z_v$ and identities everywhere else. The corresponding measurement would have X and Z in such a way that they mimic the tensor product (24). In such a case, from the inputs sent to all vertices in d -neighbourhood of u and two neighbouring vertices, all of them are ensured to measure X and Z . The simulation of the stabilizing condition equips us with relation

$$X_u \otimes_{v \in N(u)} Z_v |\Psi\rangle = |\Psi\rangle, \quad (28)$$

for $u \in V'$. Finally, the Eq.(27) and Eq.(28) ensure the existence of a local isometry mapping the physical state to the inflated graph state.

Second, for RE 5, the concept of the proof is similar to the one of RE 4. We aim to prove relations (27) and (28) which fulfill the two conditions in Proposition 1. The two observables X_u and Z_u stem from the Pauli tensor products in Eq.(25) and Eq.(26). If a PE simulates RE 2, Lemma 1 implies the existence of measurement observables \mathcal{X}_{v_0} and \mathcal{Z}_{v_0} for the vertex $v_0 \in N(v_c)$ on such that $\{\mathcal{X}_v, \mathcal{Z}_v\}|\Psi\rangle = 0$. Due to the classical communication, these variables can not replicate the stabilizer conditions in Eq.(28) since, at least on the tripoint graph, its nearest neighbour is given the measurement setting corresponding to the Pauli X operator. Using the submeasurements f_{v_0} from measurements $\tilde{M}_{v_0}^{(X)}$ in Eq.(22) and f_{v_c} from $\tilde{M}_{v_0}^{(Z)}$ in Eq.(23), we infer that $\{X_{v_c}, Z_{v_c}\}|\Psi\rangle = 0$ from $\{\mathcal{X}_{v_0}, \mathcal{Z}_{v_0}\}|\Psi\rangle = 0$ in the same way that we prove Lemma 2. In the same way, we propagate the anti-commutation relation $\{X_{v_c}, Z_{v_c}\}|\Psi\rangle = 0$ with submeasurements f_u from measurements defined by Eq.(25) and Eq.(26) to every vertex $u \in V$ of the honeycomb lattice such that $\{X_u, Z_u\}|\Psi\rangle = 0$. Equation (28) follows from the submeasurements g_u from measurements defined by Eq.(25) and Eq.(26). Finally, the Eq.(27) and Eq.(28) ensure the existence of a local isometry mapping the physical state to the honeycomb graph state.

Note that RE 5 does not depend the communication distance d , which applies if the lattice is infinite. As soon as it is finite, the stabilizer elements change at the boundaries and break the symmetry, which gives the d -LHV* model an advantage. We want to emphasize that the result from Theorem 1 and Theorem 2 are, in general, compatible that is, for a given communication distance d , they can be combined to self-test certain parts of the graph entirely while others have to be measured out.

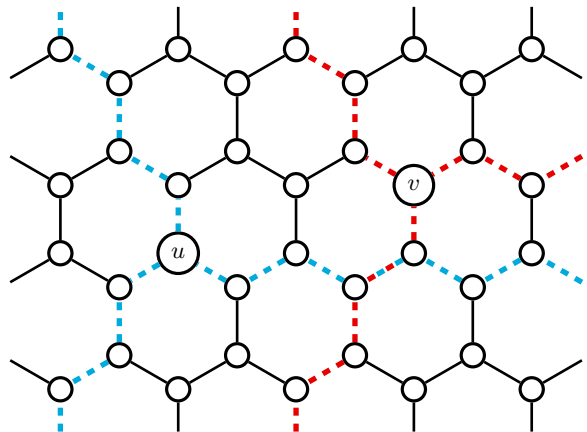


FIG. 5: We illustrate an excerpt of the honeycomb cluster. The dashed lines sketch the pattern that defines the d -inflated star graph, which we call *tripoint star*. The blue tripoint star is defined around vertex $u \in V_{hex_1}$ and the red tripoint star around vertex $v \in V_{hex_2}$, where V_{hex_1} and V_{hex_2} are the two hexagonal lattices that define the honeycomb lattice.

IV. CONCLUSION

In this work we show that it is possible to self test graph states, even when allowing for communication amongst parties. Surprisingly we show that for some graph states this can be done directly, that is, in the standard setting of self testing, but allowing communication between the devices. For our communication scenario this is not possible for all graph states, but we are able to self test them in a round about way, by preparing larger graph states and measuring them, such that they prepare the target graph state at the same time as self testing it.

In this work, the allowed communication is defined by the same graph as the state itself, this follows the original works where communication is considered for showing non-classicality [36, 41], which is motivated by the fact that it is natural that neighbours in the graph communicate in order to establish the graph state itself. One could, of course, consider different communication graphs. And indeed states which are not graph states. This would be an interesting open set of problems.

Finally, we note that another motivation for our communication scenario is that it has already found application in proving quantum advantage in computation [39, 40], communication [37] and randomness expansion [38]. Given these, and the ever increasing use of self testing to device independence in quantum technologies [48], our results offer perspectives for pushing the applications of self testing to new situations and advantage.

ACKNOWLEDGMENTS

We acknowledge funding from the ANR through the ANR-17-CE24-0035 VanQuTe project and the PEPR

integrated project EPiQ ANR-22-PETQ-0007 part of Plan France 2030.

-
- [1] John S Bell. On the Einstein Podolsky Rosen paradox. *Physics Physique Fizika*, 1:195–200, Nov 1964. doi:10.1103/PhysicsPhysiqueFizika.1.195.
- [2] Nicolas Brunner, Daniel Cavalcanti, Stefano Pironio, Valerio Scarani, and Stephanie Wehner. Bell nonlocality. *Rev. Mod. Phys.*, 86:419–478, Apr 2014. doi:10.1103/RevModPhys.86.419.
- [3] Roger Colbeck. *Quantum And Relativistic Protocols For Secure Multi-Party Computation*. PhD thesis, University of Cambridge, 2006. URL: <https://arxiv.org/abs/0911.3814>.
- [4] Roger Colbeck and Adrian Kent. Private randomness expansion with untrusted devices. *Journal of Physics A: Mathematical and Theoretical*, 44(9):095305, 2011. doi:10.1088/1751-8113/44/9/095305.
- [5] Antonio Acín and Lluís Masanes. Certified randomness in quantum physics. *Nature*, 540:213–219, 2016. doi:10.1038/nature20119.
- [6] Stefano Pironio, Antonio Acín, Serge Massar, A Boyer de La Giroday, Dzmitry N Matsukevich, Peter Maunz, Steven Olmschenk, David Hayes, Le Luo, T Andrew Manning, et al. Random numbers certified by Bell’s theorem. *Nature*, 464(7291):1021–1024, 2010. doi:10.1038/nature09008.
- [7] Antonio Acín, Nicolas Gisin, and Lluís Masanes. From bell’s theorem to secure quantum key distribution. *Phys. Rev. Lett.*, 97:120405, Sep 2006. doi:10.1103/PhysRevLett.97.120405.
- [8] Antonio Acín, Nicolas Brunner, Nicolas Gisin, Serge Massar, Stefano Pironio, and Valerio Scarani. Device-independent security of quantum cryptography against collective attacks. *Phys. Rev. Lett.*, 98:230501, Jun 2007. doi:10.1103/PhysRevLett.98.230501.
- [9] Dominic Mayers and Andrew Yao. Quantum cryptography with imperfect apparatus. In *Proceedings 39th Annual Symposium on Foundations of Computer Science (Cat. No.98CB36280)*, pages 503–509, 1998. doi:10.1109/SFCS.1998.743501.
- [10] Dominic Mayers and Andrew Yao. Self testing quantum apparatus. *Quantum Information & Computation*, 4(4):273–286, 2004. doi:10.26421/QIC4.4-3.
- [11] Ivan Šupić and Joseph Bowles. Self-testing of quantum systems: a review. *Quantum*, 4:337, September 2020. doi:10.22331/q-2020-09-30-337.
- [12] Umesh Vazirani and Thomas Vidick. Fully device independent quantum key distribution. *Commun. ACM*, 62(4):133, mar 2019. doi:10.1145/3310974.
- [13] Rotem Arnon-Friedman, Frédéric Dupuis, Omar Fawzi, Renato Renner, and Thomas Vidick. Practical device-independent quantum cryptography via entropy accumulation. *Nature communications*, 9(1):459, 2018. doi:10.1038/s41467-017-02307-4.
- [14] Rodrigo Gallego, Nicolas Brunner, Christopher Hadley, and Antonio Acín. Device-independent tests of classical and quantum dimensions. *Physical review letters*, 105(23):230501, 2010. doi:10.1103/PhysRevLett.105.230501.
- [15] Andrea Coladangelo, Alex B Grilo, Stacey Jeffery, and Thomas Vidick. Verifier-on-a-leash: new schemes for verifiable delegated quantum computation, with quasilinear resources. In *Annual international conference on the theory and applications of cryptographic techniques*, pages 247–277. Springer, 2019. doi:10.1007/978-3-030-17659-4_9.
- [16] Ben W Reichardt, Falk Unger, and Umesh Vazirani. Classical command of quantum systems. *Nature*, 496(7446):456–460, 2013. doi:10.1038/nature12035.
- [17] Jérémy Ribeiro, Gláucia Murta, and Stephanie Wehner. Fully device-independent conference key agreement. *Physical Review A*, 97(2):022307, 2018. doi:10.1103/PhysRevA.97.022307.
- [18] Kim Vallée, Pierre-Emmanuel Emeriau, Boris Bourdoncle, Adel Sohbi, Shane Mansfield, and Damian Markham. Corrected bell and noncontextuality inequalities for realistic experiments, 2023. arXiv:2310.19383.
- [19] Andreas Fyrillas, Boris Bourdoncle, Alexandre Maños, Pierre-Emmanuel Emeriau, Kayleigh Start, Nico Margaria, Martina Morassi, Aristide Lemaitre, Isabelle Sagnes, Petr Stepanov, Thi Huong Au, Sébastien Boissier, Niccolò Somaschi, Nicolas Maring, Nadia Belabas, and Shane Mansfield. Certified randomness in tight space, 2023. arXiv:2301.03536.
- [20] Gláucia Murta and Flavio Baccari. Self-testing with dishonest parties and device-independent entanglement certification in quantum communication networks. *Phys. Rev. Lett.*, 131:140201, Oct 2023. doi:10.1103/PhysRevLett.131.140201.
- [21] Richard Cleve, Peter Hoyer, Benjamin Toner, and John Watrous. Consequences and limits of nonlocal strategies. In *Proceedings. 19th IEEE Annual Conference on Computational Complexity, 2004.*, pages 236–249. IEEE, 2004. doi:10.1109/CCC.2004.1313847.
- [22] Robert Raussendorf and Hans J. Briegel. A one-way quantum computer. *Phys. Rev. Lett.*, 86:5188–5191, May 2001. doi:10.1103/PhysRevLett.86.5188.
- [23] Sara Bartolucci, Patrick Birchall, Hector Bombin, Hugo Cable, Chris Dawson, Mercedes Gimeno-Segovia, Eric Johnston, Konrad Kieling, Naomi Nickerson, Mihir Pant, et al. Fusion-based quantum computation. *Nature Communications*, 14(1):912, 2023. doi:10.1038/s41467-023-36493-1.
- [24] Daniel Gottesman. Stabilizer codes and quantum error correction. *Ph. D. thesis, California Institute of Technology*, 1997. URL: <https://thesis.library.caltech.edu/2900/2/THESIS.pdf>.
- [25] Robert Raussendorf, Jim Harrington, and Kovid Goyal. A fault-tolerant one-way quantum computer. *Annals of physics*, 321(9):2242–2270, 2006. doi:10.1016/j.aop.2006.01.012.

- [26] Nathan Shettell and Damian Markham. Graph states as a resource for quantum metrology. *Phys. Rev. Lett.*, 124:110502, Mar 2020. doi:10.1103/PhysRevLett.124.110502.
- [27] Damian Markham and Barry C. Sanders. Graph states for quantum secret sharing. *Phys. Rev. A*, 78:042309, Oct 2008. doi:10.1103/PhysRevA.78.042309.
- [28] Matthias Christandl and Stephanie Wehner. Quantum anonymous transmissions. In *International conference on the theory and application of cryptology and information security*, pages 217–235. Springer, 2005. doi:10.1007/11593447_12.
- [29] Chao-Yang Lu, Xiao-Qi Zhou, Otfried Gühne, Wei-Bo Gao, Jin Zhang, Zhen-Sheng Yuan, Alexander Goebel, Tao Yang, and Jian-Wei Pan. Experimental entanglement of six photons in graph states. *Nature physics*, 3(2):91–95, 2007. doi:10.1038/nphys507.
- [30] Ido Schwartz, Dan Cogan, Emma R Schmidgall, Yaroslav Don, Liron Gantz, Oded Kenneth, Netanel H Lindner, and David Gershoni. Deterministic generation of a cluster state of entangled photons. *Science*, 354(6311):434–437, 2016. doi:10.1126/science.aah4758.
- [31] D Istrati, Y Pilnyak, JC Loredó, C Antón, N Somaschi, P Hilaire, H Ollivier, M Esmann, L Cohen, L Vidro, et al. Sequential generation of linear cluster states from a single photon emitter. *Nature communications*, 11(1):5501, 2020. doi:10.1038/s41467-020-19341-4.
- [32] Bryn A Bell, DA Herrera-Martí, MS Tame, Damian Markham, WJ Wadsworth, and JG Rarity. Experimental demonstration of a graph state quantum error-correction code. *Nature communications*, 5(1):3658, 2014. doi:10.1038/ncomms4658.
- [33] BA Bell, Damian Markham, DA Herrera-Martí, Anne Marin, WJ Wadsworth, JG Rarity, and MS Tame. Experimental demonstration of graph-state quantum secret sharing. *Nature communications*, 5(1):1–12, 2014. doi:10.1038/ncomms6480.
- [34] Otfried Gühne, Géza Tóth, Philipp Hyllus, and Hans J. Briegel. Bell inequalities for graph states. *Phys. Rev. Lett.*, 95:120405, Sep 2005. doi:10.1103/PhysRevLett.95.120405.
- [35] Géza Tóth, Otfried Gühne, and Hans J. Briegel. Two-setting bell inequalities for graph states. *Phys. Rev. A*, 73:022303, Feb 2006. doi:10.1103/PhysRevA.73.022303.
- [36] Jonathan Barrett, Carlton M. Caves, Bryan Eastin, Matthew B. Elliott, and Stefano Pironio. Modeling Pauli measurements on graph states with nearest-neighbor classical communication. *Phys. Rev. A*, 75:012103, Jan 2007. doi:10.1103/PhysRevA.75.012103.
- [37] François Le Gall, Harumichi Nishimura, and Ansis Rosmanis. Quantum Advantage for the LOCAL Model in Distributed Computing. In Rolf Niedermeier and Christophe Paul, editors, *36th International Symposium on Theoretical Aspects of Computer Science (STACS 2019)*, volume 126 of *Leibniz International Proceedings in Informatics (LIPIcs)*, pages 49:1–49:14, Dagstuhl, Germany, 2019. Schloss Dagstuhl–Leibniz-Zentrum fuer Informatik. doi:10.4230/LIPIcs.STACS.2019.49.
- [38] Matthew Coudron, Jalex Stark, and Thomas Vidick. Trading locality for time: certifiable randomness from low-depth circuits. *Communications in mathematical physics*, 382(1):49–86, 2021. doi:10.1007/s00220-021-03963-w.
- [39] Sergey Bravyi, David Gosset, Robert Koenig, and Marco Tomamichel. Quantum advantage with noisy shallow circuits. *Nature Physics*, 16(10):1040–1045, 2020. doi:10.1038/s41567-020-0948-z.
- [40] Sergey Bravyi, David Gosset, and Robert König. Quantum advantage with shallow circuits. *Science*, 362(6412):308–311, 2018. doi:10.1126/science.aar3106.
- [41] Uta Isabella Meyer, Frédéric Grosshans, and Damian Markham. Inflated graph states refuting communication-assisted local-hidden-variable models. *Physical Review A*, 108, 2023. doi:10.1103/PhysRevA.108.012402.
- [42] Matthew McKague. Self-testing graph states. In *Conference on Quantum Computation, Communication, and Cryptography*, pages 104–120. Springer, 2011. doi:10.1007/978-3-642-54429-3_7.
- [43] Valerio Scarani, Antonio Acín, Emmanuel Schenck, and Markus Aspelmeyer. Nonlocality of cluster states of qubits. *Phys. Rev. A*, 71:042325, 4 2005. doi:10.1103/PhysRevA.71.042325.
- [44] Matthew McKague. Interactive proofs for BQP via self-tested graph states. *Theory of Computing*, 12(3):1–42, 2016. doi:10.4086/toc.2016.v012a003.
- [45] Daniel M Greenberger, Michael A Horne, Abner Shimony, and Anton Zeilinger. Bell’s theorem without inequalities. *American Journal of Physics*, 58(12):1131–1143, 1990. doi:10.1119/1.16243.
- [46] Marc Hein, Jens Eisert, and Hans J Briegel. Multiparty entanglement in graph states. *Physical Review A*, 69(6):062311, 2004. doi:10.1103/PhysRevA.69.062311.
- [47] John F. Clauser, Michael A. Horne, Abner Shimony, and Richard A. Holt. Proposed experiment to test local hidden-variable theories. *Phys. Rev. Lett.*, 23:880–884, Oct 1969. doi:10.1103/PhysRevLett.23.880.
- [48] Ivan Šupić, Andrea Coladangelo, Remigiusz Augusiak, and Antonio Acín. Self-testing multipartite entangled states through projections onto two systems. *New journal of Physics*, 20(8):083041, 2018. doi:10.1088/1367-2630/aad89b.
- [49] F. Baccari, R. Augusiak, I. Šupić, J. Tura, and A. Acín. Scalable bell inequalities for qubit graph states and robust self-testing. *Phys. Rev. Lett.*, 124:020402, Jan 2020. URL: <https://link.aps.org/doi/10.1103/PhysRevLett.124.020402>, doi:10.1103/PhysRevLett.124.020402.
- [50] Cédric Bamps and Stefano Pironio. Sum-of-squares decompositions for a family of Clauser-Horne-Shimony-Holt-like inequalities and their application to self-testing. *Phys. Rev. A*, 91:052111, May 2015. doi:10.1103/PhysRevA.91.052111.

Appendix A: Novel reference experiment for graph states

We present a new reference experiment (RE) using Pauli measurements on graph states whose corresponding graph contains an induced subgraph with three vertices in a line. Here, we give a proof for an ideal self-test, $\epsilon, \delta \rightarrow 0$ in Def. 4, and show its robustness, $\delta \sim \mathcal{O}(\sqrt{\epsilon})$ in Appendix F. For a set U of vertices, we denote $N(U) = \bigcap_{u \in U} N(u)$ as the intersection of all nearest neighborhoods of the vertices in the subset.

Reference Experiment 6 (Line of three vertices). *Let $G = (V, E)$ be a graph with an induced subgraph of three vertices $\{v_l, v_c, v_r\}$ in a line $(v_l, v_c), (v_r, v_c) \in E$ and $(v_l, v_r) \notin E$. The reference experiment consists of the corresponding graph state $|\psi\rangle$, the Pauli measurements corresponding to the generator elements $g_u = X_u Z^{N(u)}$ for every vertex $u \in V$, $M_v = Y_{v_c} Y_v Z^{N(\{v_c, v\})}$ for all $v \in N(v_c)$, and $M_{v_c} = Y_{v_l} X_{v_c} Y_{v_r} Z^{N(\{v_l, v_c, v_r\})}$.*

Theorem 3. *If a physical experiment is compatible and ϵ -simulates in terms of Def. 2 the reference experiment 6, they are δ -equivalent in terms of Def. 4.*

Proof for $\epsilon, \delta = 0$. The first step is to exploit all the implications from the conditions that a PE is *compatible* and *ϵ -simulates* the reference experiment 6.

We determine the expectation values of the RE's measurements by writing them in terms of the graph state's generator elements. Given that $M_{v_c} = -g_{v_l} g_{v_c} g_{v_r}$ and $M_v = g_{v_c} g_v$, the expectation values are $(-1) \mathbb{E}_{|\psi\rangle}(M_{v_c}) = \mathbb{E}_{|\psi\rangle}(M_v) = \mathbb{E}_{|\psi\rangle}(g_u) = 1$, for all $u \in V$ and $v \in N(v_c)$. Since the expectation values are equal to ± 1 , the measurements have deterministic outcomes and we can deduce that $(-1) M_{v_c} |\psi\rangle = M_v |\psi\rangle = g_u |\psi\rangle = |\psi\rangle$.

Consider a PE that simulates the RE, with state $|\Psi\rangle$ and measurements ξ_u for $u \in V$, \mathcal{M}_v for $v \in N(v_c)$, and \mathcal{M}_{v_c} , where ξ_u represents the PE's measurement correlations corresponding to the generator element g_u in the RE. We also use calligraphic font for the observables of the PE in contrast to italic font for the RE. Then, $\xi_u = \mathcal{X}_u Z^{N(u)}$, $\mathcal{M}_v = \mathcal{Y}_{v_c} \mathcal{Y}_v Z^{N(\{v_c, v\})}$, and $\mathcal{M}_{v_c} = \mathcal{Y}_{v_l} \mathcal{X}_{v_c} \mathcal{Y}_{v_r} Z^{N(\{v_l, v_c, v_r\})}$. Recall that we do not assume anything about the observables of the PE but that they are defined over the same Hilbert space as the ones from the RE. Since the PE simulates the RE, the measurement outcome are also deterministically equal to ± 1 , and $O^2 = \mathbb{1}$ for all occurring local operators O . Furthermore, $(-1) \mathcal{M}_{v_c} |\Psi\rangle = \mathcal{M}_u |\Psi\rangle = \xi_w |\Psi\rangle = |\Psi\rangle$. so that $\mathcal{X}_u Z^{N(u)} |\Psi\rangle = |\Psi\rangle$ and $\mathcal{Y}_{v_c} \mathcal{Y}_v Z^{N(\{v_c, u\})} |\Psi\rangle = |\Psi\rangle$, and in particular,

$$\begin{array}{llll} \mathcal{Y}_{v_l} \mathcal{X}_{v_c} \mathcal{Y}_{v_r} Z^{N(\{v_l, v_c, v_r\})} & |\Psi\rangle = & -|\Psi\rangle, \\ \mathcal{Y}_{v_l} \mathcal{Y}_{v_c} \mathcal{Z}_{v_r} Z^{N(\{v_l, v_c\}) \setminus \{v_r\}} & |\Psi\rangle = & |\Psi\rangle, \\ \mathcal{Z}_{v_l} \mathcal{X}_{v_c} \mathcal{Z}_{v_r} Z^{N(v_c) \setminus \{v_l, v_r\}} & |\Psi\rangle = & |\Psi\rangle, \\ \mathcal{Z}_{v_l} \mathcal{Y}_{v_c} \mathcal{Y}_{v_r} Z^{N(\{v_c, v_r\}) \setminus \{v_l\}} & |\Psi\rangle = & |\Psi\rangle. \end{array}$$

By applying these relations in sequence, we now prove anti-commutation relations in terms of their action on the state $|\Psi\rangle$ for two observables of each vertex. For vertex v_c , $(-1) |\Psi\rangle = \mathcal{M}_{v_c} \mathcal{M}_{v_l} \xi_{v_c} \mathcal{M}_{v_r} |\Psi\rangle = \mathcal{X}_{v_l} \mathcal{Y}_{v_c} \mathcal{Y}_{v_l} \mathcal{X}_{v_l} |\Psi\rangle$ implies $\{\mathcal{X}_{v_c}, \mathcal{Y}_{v_c}\} |\Psi\rangle = 0$. The calculus can be visualized with the above array of relations by multiplying the observables from top to bottom for every vertex.

With $\mathcal{M}_v \xi_{v_c} \mathcal{M}_v \xi_{v_c} |\Psi\rangle = |\Psi\rangle$ this anti-commutation relation propagates to one for every $v \in N(v_c)$. As above, it is easy to evaluate by writing the observables row-wise and them multiply column-wise, namely

$$\begin{array}{llll} \mathcal{Z}_v \mathcal{X}_{v_c} Z^{N(v_c) \setminus \{v\}} & |\Psi\rangle = & -|\Psi\rangle, \\ \mathcal{Y}_v \mathcal{Y}_{v_c} Z^{N(\{v, v_c\})} & |\Psi\rangle = & |\Psi\rangle, \\ \mathcal{Z}_v \mathcal{X}_{v_c} Z^{N(v_c) \setminus \{v\}} & |\Psi\rangle = & -|\Psi\rangle, \\ \mathcal{Y}_v \mathcal{Y}_{v_c} Z^{N(\{v, v_c\})} & |\Psi\rangle = & |\Psi\rangle. \end{array}$$

It follows from $\{\mathcal{X}_{v_c}, \mathcal{Y}_{v_c}\} |\Psi\rangle = 0$ that $\{\mathcal{Y}_v, \mathcal{Z}_v\} |\Psi\rangle = 0$. We write $|\Psi\rangle = \xi_w \mathcal{M}_v \xi_w \mathcal{M}_v |\Psi\rangle$ in an array,

$$\begin{array}{llll} \mathcal{X}_w \mathcal{Z}_v Z^{N(w) \setminus \{v\}} & |\Psi\rangle = & |\Psi\rangle, \\ \mathcal{Z}_w \mathcal{Y}_v \mathcal{Y}_{v_c} Z^{N(\{v, v_c\}) \setminus \{w\}} & |\Psi\rangle = & |\Psi\rangle, \\ \mathcal{X}_w \mathcal{Z}_v Z^{N(w) \setminus \{v\}} & |\Psi\rangle = & |\Psi\rangle, \\ \mathcal{Z}_w \mathcal{Y}_v \mathcal{Y}_{v_c} Z^{N(\{v, v_c\}) \setminus \{w\}} & |\Psi\rangle = & |\Psi\rangle. \end{array}$$

to visualize that it implies $\{\mathcal{X}_w, \mathcal{Z}_w\} |\Psi\rangle = 0$ for every vertex $w \in N(v) \setminus \{v_c\}$ from the previous anti-commutation relation.

For all other vertices, one sequentially applies Lemma 2 from [42] that propagates the anti-commutation relation from a vertex $w \in N(u)$ with $\{\mathcal{X}_w, \mathcal{Z}_w\} |\Psi\rangle = 0$ to any other vertex u such that $\{\mathcal{X}_u, \mathcal{Z}_u\} |\Psi\rangle = 0$ using $\xi_w \xi_u \xi_w \xi_u |\psi\rangle = |\psi\rangle$. Again, writing the measurements in an array can help visually verify this.

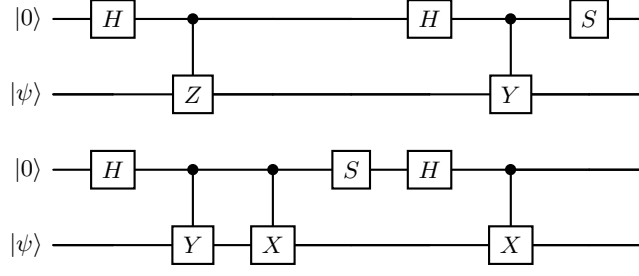


FIG. 6: As an alternative to the quantum circuit in Fig. 1, each quantum circuit implements a SWAP gate between an input state $|\psi\rangle$ and the state $|0\rangle$ with the Hadamard gate H and Pauli operators X, Y, Z .

Note that one can obtain an anti-commutation relation $\{\mathcal{X}, \mathcal{Z}\}|\Psi\rangle = 0$ for all vertices in particular for $v \in N(v_c)$ and v_c in exchange for measuring on these vertices in a third Pauli basis if the graph consists of more than three vertices. Specifically, if a vertex $u \in N(N(v_c))$ exists, then we have shown that $\{\mathcal{X}_u, \mathcal{Z}_u\}|\Psi\rangle = 0$, and using the Lemma 2 in [42], we can back-propagate the anti-commutation relation to these vertices. In this case, the following isometry is slightly easier to evaluate because it is equivalent to the one used in [42].

We demonstrate the equivalence between the PE and the RE using all the implications arising from the PE simulating the RE.

The local isometry for Def. 3 is $\phi = \prod_{u \in V} \phi_u$, with ϕ_u defined by one of the circuits in Fig. 1 and Fig. 6. The choice of circuit (i.e., operators) depends on the observables in the reference experiment. Including the respective ancilla qubits, we apply the third circuit to the vertex v_c , the second circuit to all neighbor vertices $u \in N(v_c)$ of the vertex v_c , and the first circuit to all other vertices.

For brevity, we define the corresponding operators $\mathcal{O}_u = \mathcal{X}_u$ for $u \in V \setminus N(v_c)$, $\mathcal{O}_u = i\mathcal{Y}_u$ for $u \in N(v_c)$, and $\bar{\mathcal{Z}}_u := (\bar{\mathcal{Z}}_0)_u = (\mathbf{1}_u + \mathcal{Z}_u)/2$ for $u \in V \setminus \{v_c\}$ and $\mathcal{Z}_{v_c} := (\bar{\mathcal{Z}}_0)_{v_c} = (\mathbf{1}_{v_c} + i\mathcal{Y}_{v_c}\mathcal{X}_{v_c})/2$. Using the anti-commutation relations, we obtain $\mathcal{O}_u^{a_u}(\bar{\mathcal{Z}}_{a_u})_u|\psi\rangle = \bar{\mathcal{Z}}_u\mathcal{O}_u^{a_u}|\psi\rangle$. As a result, the isometry's action is

$$\phi(|\mathbf{0}\rangle \otimes |\psi\rangle) = \bigotimes_{u \in V} \sum_{a_u=0,1} |a_u\rangle \otimes \mathcal{O}_u^{a_u}(\bar{\mathcal{Z}}_{a_u})_u|\psi\rangle = \sum_{\mathbf{a} \in \mathbb{F}_2^{|V|}} |\mathbf{a}\rangle \bigotimes_{u \in V} \mathcal{O}_u^{a_u}(\bar{\mathcal{Z}}_{a_u})_u|\psi\rangle = \sum_{\mathbf{a} \in \mathbb{F}_2^{|V|}} |\mathbf{a}\rangle \bigotimes_{u \in V} \bar{\mathcal{Z}}_u \mathcal{O}_u^{a_u}|\psi\rangle. \quad (\text{A1})$$

For further evaluation, we denote $V' = V \setminus (N(v_c) \cup \{v_c\})$. Additionally, consider some fixed but arbitrary order of the vertices $N(v_c)$ and V' which justify the notation $u < v$ for two ordered vertices u, v . Then,

$$\phi(|\mathbf{0}\rangle \otimes |\psi\rangle) = \sum_{\mathbf{a} \in \mathbb{F}_2^{|V|}} |\mathbf{a}\rangle \bigotimes_{u \in V} \bar{\mathcal{Z}}_u \mathcal{O}_u^{a_u}|\psi\rangle \quad (\text{A2})$$

$$= \frac{1}{2^{|V|}} \sum_{\mathbf{a} \in \mathbb{F}_2^{|V|}} |\mathbf{a}\rangle \otimes \left[(\mathbf{1}_{v_c} + i\mathcal{Y}_{v_c}\mathcal{X}_{v_c}) \mathcal{X}_{v_c}^{a_{v_c}} \bigotimes_{u \in N(v_c)} (\mathbf{1}_u + \mathcal{Z}_u) (i\mathcal{Y}_u)^{a_u} \bigotimes_{v \in V'} (\mathbf{1}_v + \mathcal{Z}_v) \mathcal{X}_v^{a_v} |\psi\rangle \right] \quad (\text{A3})$$

$$= \sum_{\mathbf{a} \in \mathbb{F}_2^{|V|}} |\mathbf{a}\rangle \bigotimes_{\substack{u \in N(v_c) \\ v \in V'}} (-1)^{a_u a_v \delta(v \in N(u))} \prod_{u < w \in N(v_c)} (-1)^{a_u a_w} \left[\bar{\mathcal{Z}}_{v_c} \bar{\mathcal{Z}}_u \bar{\mathcal{Z}}_v \mathcal{X}_{v_c}^{a_{v_c}} (i\mathcal{Y}_{v_c})^{a_u} \mathcal{X}_v^{a_v} |\Psi\rangle \right] \quad (\text{A4})$$

$$= \sum_{\mathbf{a} \in \mathbb{F}_2^{|V|}} |\mathbf{a}\rangle \bigotimes_{\substack{u \in N(v_c) \\ v \in V'}} (-1)^{a_u a_{v_c} + a_u a_v \delta(v \in N(u))} \prod_{\substack{u < w \in N(v_c) \\ v < w}} (-1)^{a_u a_w} \left[\bar{\mathcal{Z}}_{v_c} \bar{\mathcal{Z}}_u \bar{\mathcal{Z}}_v |\Psi\rangle \right] \quad (\text{A5})$$

$$:= \sum_{\mathbf{a} \in \mathbb{F}_2^{|V|}} (-1)^{g'(\mathbf{a})} |\mathbf{a}\rangle \bigotimes_{\substack{u \in N(v_c) \\ v \in V'}} \left[\bar{\mathcal{Z}}_{v_c} \bar{\mathcal{Z}}_u \bar{\mathcal{Z}}_v |\Psi\rangle \right], \quad (\text{A6})$$

with $g'(\mathbf{a}) = \sum_{u \in N(v_c)} a_u a_{v_c} + \sum_{\substack{v \in V' \\ v < w \in V}} a_v a_w \delta(w \in N(v)) + \sum_{u, w \in N(v_c)} a_u a_w$.

For Eq. (A3) choose an arbitrary but fixed order of the vertices $u \in N(v_c)$ and apply the following three steps sequentially for every vertex. First, we use $\mathcal{M}_u|\Psi\rangle = |\Psi\rangle$ as $\mathcal{Y}_u^{a_u}|\Psi\rangle = (\mathcal{Z}^{N(\{v_c, u\})}\mathcal{Y}_{v_c})^{a_u}|\Psi\rangle$, then the anti-commutation relation $\mathcal{Z}_v^{a_v}\mathcal{Y}_v^{a_v}|\Psi\rangle = (-1)^{a_u a_v}\mathcal{Y}_v^{a_v}\mathcal{Z}_v^{a_u}|\Psi\rangle$ for all remaining $u \in N(v_c)$ and, third, $(\mathbf{1}_v + \mathcal{Z}_v)\mathcal{Z}_v^{a_u} = (\mathbf{1}_v + \mathcal{Z}_v)$.

For Eq. (A4), we anti-commute $\mathcal{X}_{v_c}^{a_{v_c}}$, $\mathcal{Y}_{v_c}^{a_u}$, and absorb $(\mathbb{1}_{v_c} + i\mathcal{Y}_{v_c}\mathcal{X}_{v_c})(i\mathcal{Y}_{v_c})^{a_u} = (\mathbb{1}_{v_c} + i\mathcal{Y}_{v_c}\mathcal{X}_{v_c})\mathcal{X}_{v_c}^{a_u}$ for every $u \in N(v_c)$.

For Eq. (A5), we apply $\mathcal{X}_{v_c}^{a_u}|\Psi\rangle = (\mathcal{Z}^{N(v_c)})^{a_u}|\Psi\rangle$ and $\mathcal{X}_v^{a_v}|\Psi\rangle = (\mathcal{Z}^{N(v)})^{a_v}|\Psi\rangle$ for an arbitrarily fixed order of $v \in V \setminus N(v_c)$ from $\xi_v|\Psi\rangle = |\Psi\rangle$.

As a result, we obtain

$$\phi(|\mathbf{0}\rangle \otimes |\psi\rangle) = |G'\rangle \otimes |junk\rangle, \quad |junk\rangle = 2^{|V|/2} \bigotimes_{u \in V} \bar{\mathcal{Z}}_u |\Psi\rangle, \quad |G'\rangle = \sum_{\mathbf{a} \in \mathbb{F}_2^{|V|}} (-1)^{g'(\mathbf{a})} |\mathbf{a}\rangle / 2^{|V|/2}.$$

After local complementation around vertex v_c , the graph state is the one in RE 6, which can be attained by local unitary operations [46], such that

$$|G\rangle = \frac{1}{2^{|V|/2}} \sum_{\mathbf{a} \in \mathbb{F}_2^{|V|}} (-1)^{g(\mathbf{a})} |\mathbf{a}\rangle, \quad g(\mathbf{a}) = \sum_{u \in N(v_c)} a_u a_{v_c} + \sum_{\substack{v \in V' \\ v < u \in V}} a_v a_u \delta(w \in N(v)). \quad (\text{A7})$$

It remains to show that the isometry maps the measurements from the PE to the local measurements in the RE. For any vertex u , the observables are proportional to \mathcal{O}_u , $2(\bar{\mathcal{Z}}_0)_u - \mathbb{1}_u$, or a product of the two.

Applying the isometry to $\mathcal{O}_u|\psi\rangle$ changes $(\mathcal{O}_u)^{a_u} \rightarrow (\mathcal{O}_u)^{a_u+1}$ in Eq. (A2). Then, one substitutes $a_u \rightarrow a'_u = |a_u + 1\rangle$ so that $(\mathcal{O}_u)^{a_u} \rightarrow (\mathcal{O}_u)^{a'_u}$ and $|a_u\rangle \rightarrow |a'_u + 1\rangle$, which is the action of the Pauli operator X_u .

The isometry acts on $(2\bar{\mathcal{Z}}_u - \mathbb{1}_u)|\psi\rangle$ by changing $(\mathcal{O}_u)^{a_u} \rightarrow (\mathcal{O}_u)^{a_u} (2\bar{\mathcal{Z}}_u - \mathbb{1}_u)$ in Eq. (A2). We anti-commute $(\mathcal{O}_u)^{a_u} (2\bar{\mathcal{Z}}_u - \mathbb{1}_u) = (2(\bar{\mathcal{Z}}_{a_u})_u - \mathbb{1}_u) (\mathcal{O}_u)^{a_u}$. Absorbing $\bar{\mathcal{Z}}_u (\bar{\mathcal{Z}}_{a_u})_u = \delta_{a_u,1} \bar{\mathcal{Z}}_u$ leaves a phase $(2\delta_{a_u,1} - \mathbb{1}_u) = (-1)^{a_u}$ such that $|a_u\rangle \rightarrow (-1)^{a_u} |a_u\rangle$, the action of Pauli operator Z_u . The composition of the observables in \mathcal{O}_u and $2\bar{\mathcal{Z}}_u - \mathbb{1}_u$ matches the corresponding Pauli operators in the reference experiment.

We conclude that the physical experiment and the reference experiment are equivalent. \square

Appendix B: Tensor-product representation of Pauli correlations

We start by introducing some useful notation. Given a set of vertices V , we write $O^V = \bigotimes_{v \in V} O_v$ for local operators O_v . In particular, if O_v are Pauli operators, O^V describes a Pauli measurement whose outcome is a string of binary outputs from each vertex v . Furthermore, we label the chain vertices $s_{(u,v)}$ as odd ('o') if s is odd and even ('e') if s is even. If $s \leq d$, the vertex is on the left ('L'), and if $s > d$, on the right ('R') side of the chain. Figure 7 illustrates the notation. We denote the tensor products of Pauli X operators on the set of vertices for these labels as

$$X_{e,L} = \bigotimes_{s=1}^{\lfloor d/2 \rfloor} X_{2s(u,v)}, \quad X_{e,R} = \bigotimes_{s=\lceil d/2 \rceil}^d X_{(2s)(u,v)}, \quad X_{o,L} = \bigotimes_{s=1}^{\lfloor d/2 \rfloor} X_{(2s-1)(u,v)}, \quad X_{o,R} = \bigotimes_{s=\lceil d/2 \rceil}^d X_{(2s-1)(u,v)},$$

and $X_o = X_{o,L} X_{o,R}$, $X_e = X_{e,L} X_{e,R}$. A tensor product of multiple chains, given a Pauli product P over a single one, is $\bigotimes_{(u,N(u))} P = \bigotimes_{v \in N(u)} P_{(u,v)}$, for a set of V .

In the following, we use this notation to write all correlation operators from the reference experiments (REs) 1, 2, 3 in terms of tensor products. Next to them, we also write the observables that a compatible physical experiment (PE) assigns. We use calligraphic font for the measurements and observables of the PE, in contrast to italic font for the REs. We denote the measurements of the PE corresponding to the inflated generator element f_u by ζ_u . Recall that we label all measurement observables according to the local measurement setting. The information gained from the classical communication is accounted for in the superscripts. To keep these minimal, we only label the chain vertices according to the measurement setting of its nearest power vertex. This is possible since the measurement settings of the chain vertices are mostly the same, and we specifically outline if they change.

The d -inflated generator element is

$$f_u = X_u Z^{N(u)} X_e, \quad (\text{B1})$$

$$\zeta_u = \mathcal{X}_u \mathcal{Z}^{N(u)} \mathcal{X}_{e,L}^{(X)} \mathcal{X}_{e,R}^{(Z)}, \quad (\text{B2})$$

which also brings out its resemblance with the generator element of the original graph state $g_u = X_u Z^{N(u)}$. Given

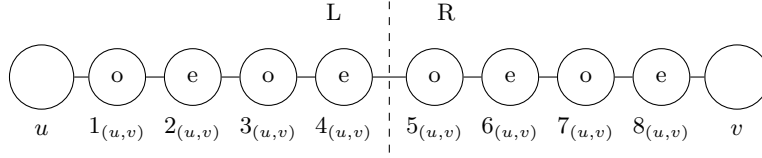


FIG. 7: For a $d = 4$ -inflated graph from two connected vertices u and v , the vertices' labels are below, and their characterization as odd (o) or even (e) inside the nodes. The chain is divided into a left (L) and right (R).

a graph $G = (V, E)$ and an induced subgraph $G_U = (U \subset V, E_U = (U \times U) \cap E)$, we define

$$S_u = Z^{N(u) \setminus U} X_{e(u, N(u) \setminus U)}, \quad (\text{B3})$$

$$\mathcal{S}_u = Z^{N(u) \setminus U} \mathcal{X}_{e,L}^{(Z)} \mathcal{X}_{e,R}^{(Z)}. \quad (\text{B4})$$

For example, if the subgraph consisting of a single vertex u , the inflated generator element can be written as $f_u = X_u S_u$.

For the reference experiment 1,

$$C_{V_c} = X^{V_c} \left(\bigotimes_{(u,v) \in E_c} X_o(u,v) X_e(u,v) \right) S^{V_c}, \quad (\text{B5})$$

$$C_w = X^{V_c \setminus (N(v) \cup \{v\})} \left(\bigotimes_{(u,v) \in E_c \setminus (w, N(w))} X_o(u,v) X_e(u,v) \right) Y^{N(w) \cap V_c} X_o(w, N(w) \cap V_c) S^{V_c \setminus \{w\}}, \quad (\text{B6})$$

and, for the PE, taking into account the round of classical communication of the measurement settings,

$$\mathcal{C}_{V_c} = \mathcal{X}^{V_c} \left(\bigotimes_{(u,v) \in E_c} \mathcal{X}_o^{(X)}(u,v) \mathcal{X}_e^{(X)}(u,v) \right) \mathcal{S}^{V_c}, \quad (\text{B7})$$

$$\mathcal{C}_w^{(X)} = \mathcal{X}^{V_c \setminus (N(v) \cup \{v\})} \left(\bigotimes_{(u,v) \in E_c \setminus (N(N(w)), N(w))} \mathcal{X}_o^{(X)}(u,v) \mathcal{X}_e^{(X)}(u,v) \right) \mathcal{Y}^{N(w) \cap V_c} \mathcal{X}_{o,L}^{(X)}(w, N(w) \cap V_c) \mathcal{X}_{o,R}^{(Y)} S^{V_c \setminus \{w\}}, \quad (\text{B8})$$

$$\mathcal{C}_w^{(Z)} = \mathcal{X}^{V_c \setminus (N(v) \cup \{v\})} \left(\bigotimes_{(u,v) \in E_c \setminus (N(N(w)), N(w))} \mathcal{X}_o^{(X)}(u,v) \mathcal{X}_e^{(X)}(u,v) \right) \mathcal{Y}^{N(w) \cap V_c} \mathcal{X}_{o,L}^{(Z)}(w, N(w) \cap V_c) \mathcal{X}_{o,R}^{(Y)} S^{V_c \setminus \{w\}}, \quad (\text{B9})$$

for all $w \in V_c$. The operators are illustrated in Fig. 4a for an exemplary graph.

For the reference experiment 2,

$$\tilde{\zeta}_{v_c} = \tilde{\mathcal{X}}_{v_c} Z^{N(v_c)} \tilde{\mathcal{X}}_{e,L}^{(X)}(v_c, N(v_c)) \tilde{\mathcal{X}}_{e,R}^{(Z)}, \quad (\text{B10})$$

and, if $|N(v_c)| > 2$,

$$C_{v_i v_j} = X_{v_c} X_{v_i} X_{v_j} Z^{N(v_c) \setminus \{v_i, v_j\}} \tilde{X}_o(v_c, v_i)(v_c, v_j)(v_c, N(v_c) \setminus \{v_i, v_j\}) \tilde{X}_e S_{v_i} S_{v_j}, \quad (\text{B11})$$

$$C_{v_i v_j} = \tilde{\mathcal{X}}_{v_c} \mathcal{X}_{v_i} \mathcal{X}_{v_j} Z^{N(v_c) \setminus \{v_i, v_j\}} \tilde{\mathcal{X}}_{o,L}^{(X)}(v_c, v_i) \tilde{\mathcal{X}}_{o,R}^{(X)}(v_c, v_j) \tilde{\mathcal{X}}_{o,L}^{(X)}(v_c, N(v_c) \setminus \{v_i, v_j\}) \tilde{\mathcal{X}}_{o,R}^{(Z)} S_{v_i} S_{v_j}, \quad (\text{B12})$$

for $V_3 = \{v_1, v_2, v_3\} \subseteq N(v_c)$ and $v_i \neq v_j$. If $N(v_c) = \{v_1, v_2\}$ such that $|N(v_c)| = 2$, for the RE

$$C_{v_c} = X_{v_c} X_{v_1} X_{v_2} \tilde{X}_{o,(v_c,v_1)} \tilde{X}_{o,(v_c,v_2)} S_{v_1} S_{v_2}, \quad (\text{B13})$$

$$C_{v_1} = Y_{v_c} X_{v_1} Z_{v_2} \tilde{X}_{o,(v_c,v_1)} \tilde{X}_{e,(v_c,v_2)} S_{v_1}, \quad (\text{B14})$$

$$C_{v_2} = Y_{v_c} Z_{v_1} X_{v_2} \tilde{X}_{e,(v_c,v_1)} \tilde{X}_{o,(v_c,v_2)} S_{v_2}, \quad (\text{B15})$$

$$C_2 = Y_{v_1} Y_{v_2} \tilde{X}_{o,(v_c,v_1)} \tilde{X}_{e,(v_c,v_1)} \tilde{X}_{o,(v_c,v_2)} \tilde{X}_{e,(v_c,v_2)} S_{v_1} S_{v_2}, \quad (\text{B16})$$

and, for the PE, taking into account the round of classical communication of the measurement settings,

$$\mathcal{C}_{v_c} = \tilde{\mathcal{X}}_{v_c} \mathcal{X}_{v_1} \mathcal{X}_{v_2} \tilde{\mathcal{X}}_{o,L}^{(X)} \tilde{\mathcal{X}}_{o,R}^{(X)} \tilde{\mathcal{X}}_{o,L}^{(X)} \tilde{\mathcal{X}}_{o,R}^{(X)} S_{v_1} S_{v_2}, \quad (\text{B17})$$

$$\mathcal{C}_{v_1} = \tilde{\mathcal{Y}}_{v_c} \mathcal{X}_{v_1} \mathcal{Z}_{v_2} \tilde{\mathcal{X}}_{o,L}^{(Y)} \tilde{\mathcal{X}}_{o,R}^{(X)} \tilde{\mathcal{X}}_{e,L}^{(Y)} \tilde{\mathcal{X}}_{e,R}^{(Z)} S_{v_1}, \quad (\text{B18})$$

$$\mathcal{C}_{v_2} = \tilde{\mathcal{Y}}_{v_c} \mathcal{Z}_{v_1} \mathcal{X}_{v_2} \tilde{\mathcal{X}}_{e,L}^{(Y)} \tilde{\mathcal{X}}_{e,R}^{(Z)} \tilde{\mathcal{X}}_{o,L}^{(Y)} \tilde{\mathcal{X}}_{o,R}^{(X)} S_{v_2}, \quad (\text{B19})$$

$$\mathcal{C}_2^{(X)} = \mathcal{Y}_{v_1} \mathcal{Y}_{v_2} \tilde{\mathcal{X}}_{o,L}^{(X)} \tilde{\mathcal{X}}_{e,L}^{(X)} \tilde{\mathcal{X}}_{o,R}^{(Y)} \tilde{\mathcal{X}}_{e,R}^{(Y)} S_{v_1} S_{v_2}, \quad (\text{B20})$$

$$\mathcal{C}_2^{(Y)} = \mathcal{Y}_{v_1} \mathcal{Y}_{v_2} \tilde{\mathcal{X}}_{o,L}^{(Y)} \tilde{\mathcal{X}}_{e,L}^{(Y)} \tilde{\mathcal{X}}_{o,R}^{(Y)} \tilde{\mathcal{X}}_{e,R}^{(Y)} S_{v_1} S_{v_2}, \quad (\text{B21})$$

The operator $\tilde{X}_{(v_c,v)}$ for every edge $(v_c, v) \in E$ is, similar to $X_{(v_c,v)}$, a tensor product of Pauli X operators but on the nearest neighbors of v_c where it has the Pauli Y operator. The operator $\tilde{\mathcal{X}}_{v_c}$ is the same as \mathcal{X}_{v_c} but accounts for the nearest neighbors of v_c measuring according to the Pauli Y operator instead of the Pauli X operator. The Pauli correlations are illustrated in Fig. 4d and Fig. 4b for exemplary graphs.

For the RE 3, the representation of measurement correlations from Eq. (10) in tensor product operators is

$$I_1 = Z_{v_l} \tilde{X}_{o,L} (R_z)_{v_m} \tilde{X}_{o,R} X_{v_r} S_{v_r}, \quad (\text{B22})$$

$$I_2 = O_{v_l} \tilde{X}_{e,L} (R_z)_{v_m} \tilde{X}_{e,R} Z_{v_r} S_{v_l}, \quad (\text{B23})$$

$$I_3 = O_{v_l} \tilde{X}_{e,L} (R_z)_{v_m} \tilde{X}_{o,R} X_{v_r} S_{v_l} S_{v_r}, \quad (\text{B24})$$

$$I_4 = Z_{v_l} \tilde{X}_{o,L} (R_z)_{v_m} \tilde{X}_{e,R} Z_{v_r}, \quad (\text{B25})$$

$$P_1 = Z_{v_l} \tilde{X}_{o,L} X_{v_m} \tilde{X}_{o,R} X_{v_r} S_{v_r}, \quad (\text{B26})$$

$$P_2 = O_{v_l} \tilde{X}_{e,L} X_{v_m} \tilde{X}_{e,R} Z_{v_r} S_{v_l}, \quad (\text{B27})$$

and, for the PE taking into account the round of classical communication of the measurement settings for the mea-

measurements \mathcal{M} ,

$$\mathcal{I}_1 = \tilde{Z}_{v_l}^{(R)} \tilde{\mathcal{X}}_{o,L}^{(Z,R)} (\tilde{\mathcal{R}}_z^{(Z)})_{v_m} \tilde{\mathcal{X}}_{o,R}^{(X,R)} \tilde{\mathcal{X}}_{v_r} \mathcal{S}_{v_r}, \quad (\text{B28})$$

$$\mathcal{I}_2 = \tilde{O}_{v_l}^{(R)} \tilde{\mathcal{X}}_{e,L}^{(O,R)} (\tilde{\mathcal{R}}_z^{(O)})_{v_m} \tilde{\mathcal{X}}_{e,R}^{(Z,R)} \tilde{Z}_{v_r} \mathcal{S}_{v_l}, \quad (\text{B29})$$

$$\mathcal{I}_3 = \tilde{O}_{v_l}^{(R)} \tilde{\mathcal{X}}_{e,L}^{(O,R)} (\tilde{\mathcal{R}}_z^{(O)})_{v_m} \tilde{\mathcal{X}}_{o,R}^{(X,R)} \tilde{\mathcal{X}}_{v_r} \mathcal{S}_{v_l} \mathcal{S}_{v_r}, \quad (\text{B30})$$

$$\mathcal{I}_4 = \tilde{Z}_{v_l}^{(R)} \tilde{\mathcal{X}}_{o,L}^{(Z,R)} (\tilde{\mathcal{R}}_z^{(Z)})_{v_m} \tilde{\mathcal{X}}_{e,R}^{(Z,R)} \tilde{Z}_{v_r}, \quad (\text{B31})$$

$$\mathcal{P}_1 = \tilde{Z}_{v_l} \tilde{\mathcal{X}}_{o,L}^{(Z)} \mathcal{X}_{v_m}^{(Z)} \tilde{\mathcal{X}}_{o,R}^{(X)} \tilde{\mathcal{X}}_{v_r} \mathcal{S}_{v_r}, \quad (\text{B32})$$

$$\mathcal{P}_2 = \tilde{O}_{v_l} \tilde{\mathcal{X}}_{e,L}^{(O)} \mathcal{X}_{v_m}^{(O)} \tilde{\mathcal{X}}_{e,R}^{(Z)} \tilde{Z}_{v_r} \mathcal{S}_{v_l}, \quad (\text{B33})$$

with $v_m := d_{(v_l, v_r)}$ and $R_z = (X + Y)/\sqrt{2}$, It is $O_{v_l} = Y_{v_l}$ if $d = 1$, and else $O_{v_l} = X_{v_l}$. The operator $\tilde{X}_{(v_l, v_r)}$ is, similar to $X_{(v_l, v_r)}$, a tensor product of Pauli X operators but on the chain vertices $(d \pm 1)_{(v_l, v_r)}$, where it has the Pauli Y operator, and on the chain vertex v_m , where it has the Pauli identity. Any observable \tilde{Q} , is the same as a corresponding observable Q but accounts for the nearest neighbors of the vertex v_m measuring according to the Pauli Y operator instead of the Pauli X operator. The operators $\mathcal{I}_1, \dots, \mathcal{I}_4$ are illustrated in Fig. 4c for an exemplary graph.

Appendix C: Proof of Lemma 1 & Lemma 2

Proof [Lemma 1, Reference experiment 1.] If the physical experiment (PE) simulates the reference experiment (RE) 1, the specified correlations from the measurements fulfill

$$\langle \Psi | \zeta_u | \Psi \rangle = 1, \quad \forall u \in V, \quad (\text{C1})$$

$$\langle \Psi | \mathcal{C}_V | \Psi \rangle = -1, \quad (\text{C2})$$

$$\langle \Psi | \mathcal{C}_v^{(X)} | \Psi \rangle = 1, \quad \forall v \in V_c, \quad (\text{C3})$$

$$\langle \Psi | \mathcal{C}_v^{(Z)} | \Psi \rangle = 1, \quad \forall v \in V_c. \quad (\text{C4})$$

Since the norm of all physical measurement observables is at most 1, Eqs. (C1)-(C4) imply

$$\zeta_u | \Psi \rangle = | \Psi \rangle, \quad \forall u \in V, \quad (\text{C5})$$

$$(-1) \mathcal{C}_V | \Psi \rangle = | \Psi \rangle, \quad (\text{C6})$$

$$\mathcal{C}_v^{(X)} | \Psi \rangle = | \Psi \rangle, \quad \forall v \in V_c, \quad (\text{C7})$$

$$\mathcal{C}_v^{(Z)} | \Psi \rangle = | \Psi \rangle, \quad \forall v \in V_c. \quad (\text{C8})$$

Recall that any vertex's observable depends on the measurement observables from all vertices $v \in N_d(u)$. In the RE one power vertex from the odd cycle does not measure any observable when the reference measurement is \mathcal{C}_v . However, as explained in the main text, whenever a vertex is not asked to measure anything in the RE, in the PE it is given an input, but the results are marginalized. Thus, physical measurement \mathcal{C}_v has two non-equivalent implementations, one in which the vertex which does not measure anything in the RE is asked to perform the measurement corresponding to X and the other in which it is asked to measure Z . We write $\mathcal{C}_v^{(X)}$ and $\mathcal{C}_v^{(Z)}$ for these two physical implementations, respectively. Both operators have congruent observables except on the chain vertices with the nearest power vertex v , thus

$$\mathcal{C}_v^{(Z)} \mathcal{C}_v^{(X)} = \mathcal{X}_{o,L}^{(Z)} \mathcal{X}_{o,L}^{(X)}. \quad (\text{C9})$$

We denote the vertices of the circular subgraph in some order along the cycle $V = \{v_1, v_2, \dots, v_{|V|}\}$ with $(v_i, v_{i\pm 1}) \in E$ and $v_{|V|+1} = v_1$, and in general $v_i = v_{i\%|V|}$. We get the following chain of relations

$$|\Psi\rangle = (-1) \mathcal{C}_V \prod_{k=1}^{|V|} \zeta_{v_{2k}} \prod_{k=1}^{|V|} \mathcal{C}_{v_{2k}}^Z \mathcal{C}_{v_{2k}}^X |\Psi\rangle \quad (\text{C10})$$

$$\begin{aligned} &= (-1) \left(\bigotimes_{k=1}^{|V|} \mathcal{X}_{v_k} \mathcal{X}_{o,L}^{(X)} \mathcal{X}_{e,L}^{(X)} \mathcal{X}_{o,R}^{(X)} \mathcal{X}_{e,R}^{(X)} \mathcal{S}_{v_k} \right) \\ &\quad \cdot \left(\bigotimes_{k=1}^{|V|} \mathcal{Z}_{v_{2k-1}} \mathcal{X}_{v_{2k}} \mathcal{Z}_{v_{2k+1}} \mathcal{X}_{o,L}^{(Z)} \mathcal{X}_{o,R}^{(X)} \mathcal{X}_{e,L}^{(X)} \mathcal{X}_{e,R}^{(Z)} \mathcal{S}_{v_{2k}} \right) \\ &\quad \cdot \left(\bigotimes_{k=1}^{|V|} \mathcal{X}_{e,R}^{(Z)} \mathcal{X}_{e,R}^{(X)} \mathcal{X}_{o,L}^{(Z)} \mathcal{X}_{o,L}^{(X)} \right) |\Psi\rangle \end{aligned} \quad (\text{C11})$$

$$\begin{aligned} &= (-1) \left(\bigotimes_{k=1}^{|V|} \mathcal{X}_{v_k} \mathcal{S}_{v_k} \right) \left(\bigotimes_{k=1}^{|V|} \mathcal{Z}_{v_{2k-1}} \mathcal{X}_{v_{2k}} \mathcal{Z}_{v_{2k+1}} \mathcal{S}_{v_{2k}} \right) \left(\bigotimes_{k=1}^{|V|} \mathcal{X}_{o,L}^{(X)} \mathcal{X}_{e,L}^{(X)} \mathcal{X}_{o,R}^{(X)} \mathcal{X}_{e,R}^{(X)} \right) \\ &\quad \cdot \left(\bigotimes_{k=1}^{|V|} \mathcal{X}_{o,L}^{(Z)} \mathcal{X}_{o,R}^{(X)} \mathcal{X}_{e,L}^{(X)} \mathcal{X}_{e,R}^{(Z)} \right) \left(\bigotimes_{k=1}^{|V|} \mathcal{X}_{e,R}^{(Z)} \mathcal{X}_{e,R}^{(X)} \mathcal{X}_{o,L}^{(Z)} \mathcal{X}_{o,L}^{(X)} \right) |\Psi\rangle \end{aligned} \quad (\text{C12})$$

$$= (-1) \left(\bigotimes_{k=1}^{|V|} \mathcal{X}_{v_k} \right) \left(\bigotimes_{k=1}^{|V|} \mathcal{Z}_{v_{2k-1}} \mathcal{X}_{v_{2k}} \mathcal{Z}_{v_{2k+1}} \right) |\Psi\rangle \quad (\text{C13})$$

$$= (-1) \mathcal{X}_{v_1} \mathcal{Z}_{v_1} \mathcal{X}_{v_1} \mathcal{Z}_{v_1} |\Psi\rangle. \quad (\text{C14})$$

Line (C10) was obtained by using Eqs. (C5)-(C8) for all $v \in V_c$. The following three lines, constituting Eq. (C11) are obtained by using Eqs. (B2), (B7)-(B9), and Eq. (C9). Line (C12) was obtained by simply rearranging the terms in the previous equation, taking care about commutation relations. Taking that the physical measurement observables square to the identity gives line (C13). There, we are only left with observables on the power vertices. We can then use the same arguments present in [42], precisely Eq. (15), on the non-inflated circle to arrive at Eq. (C14). We obtained the anti-commutation relation between observables on the power vertex v_1 .

A simple visualization of the calculus a circle with three vertices v_1, v_2, v_3 is an array whose rows contain the measurements and the deterministic outcome $\chi = \pm 1$ from $\mathcal{M}|\Psi\rangle = \chi|\Psi\rangle$. Multiplying the local observables column-wise, in reverse order of their application to the state, yields their action on the state. The Pauli measurements are products of all observables shown (in black and light-blue font). The stabilizer correlations are the products of the observables in black font with their constraints from the simulation conditions on the left. The observables in light-blue font are not considered in the calculus of the anti-commutation in Eqs. (C10)-(C14), but they are considered in the round of classical communication and thus influence the observables within communication distance.

\mathcal{M}, χ	(v_3, v_1)		v_1	(v_1, v_2)				v_2	(v_2, v_3)				v_3	(v_3, v_1)	
	o, R	e, R		o, L	e, L	o, R	e, R		o, L	e, L	o, R	e, R		o, L	e, L
$\mathcal{C}_{V_c}, -1$	$\mathcal{X}^{(X)}$	$\mathcal{X}^{(X)}$	\mathcal{X}	$\mathcal{X}^{(X)}$	$\mathcal{X}^{(X)}$	$\mathcal{X}^{(X)}$	$\mathcal{X}^{(X)}$	\mathcal{X}	$\mathcal{X}^{(X)}$	$\mathcal{X}^{(X)}$	$\mathcal{X}^{(X)}$	$\mathcal{X}^{(X)}$	\mathcal{X}	$\mathcal{X}^{(X)}$	$\mathcal{X}^{(X)}$
$\zeta_{v_2}, 1$	$\mathcal{X}^{(Z)}$	$\mathcal{X}^{(Z)}$	\mathcal{Z}	$\mathcal{X}^{(Z)}$	$\mathcal{X}^{(Z)}$	$\mathcal{X}^{(X)}$	$\mathcal{X}^{(X)}$	\mathcal{X}	$\mathcal{X}^{(X)}$	$\mathcal{X}^{(X)}$	$\mathcal{X}^{(Z)}$	$\mathcal{X}^{(Z)}$	\mathcal{Z}	$\mathcal{X}^{(Z)}$	$\mathcal{X}^{(Z)}$
$\zeta_{v_1}, 1$	$\mathcal{X}^{(X)}$	$\mathcal{X}^{(X)}$	\mathcal{X}	$\mathcal{X}^{(X)}$	$\mathcal{X}^{(X)}$	$\mathcal{X}^{(Z)}$	$\mathcal{X}^{(Z)}$	\mathcal{Z}	$\mathcal{X}^{(Z)}$	$\mathcal{X}^{(Z)}$	$\mathcal{X}^{(Z)}$	$\mathcal{X}^{(Z)}$	\mathcal{Z}	$\mathcal{X}^{(Z)}$	$\mathcal{X}^{(Z)}$
$\zeta_{v_3}, 1$	$\mathcal{X}^{(Z)}$	$\mathcal{X}^{(Z)}$	\mathcal{Z}	$\mathcal{X}^{(Z)}$	$\mathcal{X}^{(Z)}$	$\mathcal{X}^{(Z)}$	$\mathcal{X}^{(Z)}$	\mathcal{Z}	$\mathcal{X}^{(Z)}$	$\mathcal{X}^{(Z)}$	$\mathcal{X}^{(X)}$	$\mathcal{X}^{(X)}$	\mathcal{X}	$\mathcal{X}^{(X)}$	$\mathcal{X}^{(X)}$
$\mathcal{C}_{v_2}^{(Z)}, 1$	$\mathcal{X}^{(Y)}$	$\mathcal{X}^{(Y)}$	\mathcal{Y}	$\mathcal{X}^{(Y)}$	$\mathcal{X}^{(Y)}$	$\mathcal{X}^{(Z)}$	$\mathcal{X}^{(Z)}$	\mathcal{Z}	$\mathcal{X}^{(Z)}$	$\mathcal{X}^{(Z)}$	$\mathcal{X}^{(Y)}$	$\mathcal{X}^{(Y)}$	\mathcal{Y}	$\mathcal{X}^{(Y)}$	$\mathcal{X}^{(Y)}$
$\mathcal{C}_{v_2}^{(X)}, 1$	$\mathcal{X}^{(Y)}$	$\mathcal{X}^{(Y)}$	\mathcal{Y}	$\mathcal{X}^{(Y)}$	$\mathcal{X}^{(Y)}$	$\mathcal{X}^{(X)}$	$\mathcal{X}^{(X)}$	\mathcal{X}	$\mathcal{X}^{(X)}$	$\mathcal{X}^{(X)}$	$\mathcal{X}^{(Y)}$	$\mathcal{X}^{(Y)}$	\mathcal{Y}	$\mathcal{X}^{(Y)}$	$\mathcal{X}^{(Y)}$
$\mathcal{C}_{v_1}^{(Z)}, 1$	$\mathcal{X}^{(Z)}$	$\mathcal{X}^{(Z)}$	\mathcal{Z}	$\mathcal{X}^{(Z)}$	$\mathcal{X}^{(Z)}$	$\mathcal{X}^{(Y)}$	$\mathcal{X}^{(Y)}$	\mathcal{Y}	$\mathcal{X}^{(Y)}$	$\mathcal{X}^{(Y)}$	$\mathcal{X}^{(Y)}$	$\mathcal{X}^{(Y)}$	\mathcal{Y}	$\mathcal{X}^{(Y)}$	$\mathcal{X}^{(Y)}$
$\mathcal{C}_{v_1}^{(X)}, 1$	$\mathcal{X}^{(X)}$	$\mathcal{X}^{(X)}$	\mathcal{X}	$\mathcal{X}^{(X)}$	$\mathcal{X}^{(X)}$	$\mathcal{X}^{(Y)}$	$\mathcal{X}^{(Y)}$	\mathcal{Y}	$\mathcal{X}^{(Y)}$	$\mathcal{X}^{(Y)}$	$\mathcal{X}^{(Y)}$	$\mathcal{X}^{(Y)}$	\mathcal{Y}	$\mathcal{X}^{(Y)}$	$\mathcal{X}^{(Y)}$
$\mathcal{C}_{v_3}^{(Z)}, 1$	$\mathcal{X}^{(Y)}$	$\mathcal{X}^{(Y)}$	\mathcal{Y}	$\mathcal{X}^{(Y)}$	$\mathcal{X}^{(Y)}$	$\mathcal{X}^{(Y)}$	$\mathcal{X}^{(Y)}$	\mathcal{Y}	$\mathcal{X}^{(Y)}$	$\mathcal{X}^{(Y)}$	$\mathcal{X}^{(Z)}$	$\mathcal{X}^{(Z)}$	\mathcal{Z}	$\mathcal{X}^{(Z)}$	$\mathcal{X}^{(Z)}$
$\mathcal{C}_{v_3}^{(X)}, 1$	$\mathcal{X}^{(Y)}$	$\mathcal{X}^{(Y)}$	\mathcal{Y}	$\mathcal{X}^{(Y)}$	$\mathcal{X}^{(Y)}$	$\mathcal{X}^{(Y)}$	$\mathcal{X}^{(Y)}$	\mathcal{Y}	$\mathcal{X}^{(Y)}$	$\mathcal{X}^{(Y)}$	$\mathcal{X}^{(X)}$	$\mathcal{X}^{(X)}$	\mathcal{X}	$\mathcal{X}^{(X)}$	$\mathcal{X}^{(X)}$

Note that, as the odd cycle has translation symmetry, by relabeling the vertices in the proof, we can obtain the

anti-commutation relations for all power vertices belonging to the odd cycle: For all $k = 1, \dots, |V|$, we can obtain

$$\{\mathcal{X}_{v_k}, \mathcal{Z}_{v_k}\}|\Psi\rangle = 0. \quad (\text{C15})$$

By applying Lemma 2, we obtain the same anti-commutation relation for all power vertices in the inflated graph. This is possible, even if we only consider the anti-commutation relation on the power vertex v_1 \square

Proof [Lemma 1, Reference experiment 2.] If the physical experiment (PE) simulates the reference experiment (RE) 2 for $|N(v_c)| > 2$, the specified correlations from the measurements fulfill

$$\langle \Psi | \zeta_u | \Psi \rangle = 1, \quad \forall u \in V, \quad (\text{C16})$$

$$\langle \Psi | \tilde{\zeta}_{v_c} | \Psi \rangle = 1, \quad (\text{C17})$$

$$\langle \Psi | \mathcal{C}_{v_i v_j} | \Psi \rangle = -1, \quad \forall v_i \neq v_j \wedge v_i, v_j \in V_3 = \{v_1, v_2, v_3\} \subseteq N(v_c). \quad (\text{C18})$$

Since the norm of all physical measurement observables is at most 1, Eqs. (C16)-(C18) imply

$$\zeta_u | \Psi \rangle = | \Psi \rangle, \quad \forall u \in V, \quad (\text{C19})$$

$$\tilde{\zeta}_{v_c} | \Psi \rangle = | \Psi \rangle, \quad (\text{C20})$$

$$(-1) \mathcal{C}_{v_i v_j} | \Psi \rangle = | \Psi \rangle, \quad \forall v_i \neq v_j \wedge v_i, v_j \in V_3 = \{v_1, v_2, v_3\} \subseteq N(v_c). \quad (\text{C21})$$

Recall that any vertex's observable depends on the measurement observables from all vertices $v \in N_d(u)$. As explained in the main text, whenever a vertex is not asked to measure anything in the RE, in the PE it is given an input, but the results are marginalized.

Then, we get the following chain of relations

$$|\Psi\rangle = (-1) \tilde{\zeta}_{v_c} \mathcal{C}_{v_1 v_2} \mathcal{C}_{v_2 v_3} \mathcal{C}_{v_1 v_3} |\Psi\rangle \quad (\text{C22})$$

$$= (-1) \tilde{\mathcal{X}}_{v_c} \mathcal{Z}_{v_1} \mathcal{Z}_{v_2} \mathcal{Z}_{v_3} \mathcal{Z}^{N(v_c) \setminus V_3} \begin{matrix} \tilde{\mathcal{X}}_{e,L}^{(X)} \tilde{\mathcal{X}}_{e,R}^{(Z)} \\ (v_c, N(v_c)) \end{matrix} \cdot \tilde{\mathcal{X}}_{v_c} \mathcal{X}_{v_1} \mathcal{X}_{v_2} \mathcal{Z}_{v_2} \mathcal{Z}^{N(v_c) \setminus V_3} \begin{matrix} \tilde{\mathcal{X}}_{o,L}^{(X)} \tilde{\mathcal{X}}_{o,R}^{(X)} \tilde{\mathcal{X}}_{o,L}^{(X)} \tilde{\mathcal{X}}_{o,R}^{(X)} \\ (v_c, v_1) \quad (v_c, v_2) \end{matrix} \begin{matrix} \tilde{\mathcal{X}}_{e,L}^{(X)} \tilde{\mathcal{X}}_{e,R}^{(Z)} \\ (v_c, N(v_c) \setminus \{v_1, v_2\}) \end{matrix} \mathcal{S}_{v_1} \mathcal{S}_{v_2}$$

$$\cdot \tilde{\mathcal{X}}_{v_c} \mathcal{Z}_{v_1} \mathcal{X}_{v_2} \mathcal{X}_{v_3} \mathcal{Z}^{N(v_c) \setminus V_3} \begin{matrix} \tilde{\mathcal{X}}_{o,L}^{(X)} \tilde{\mathcal{X}}_{o,R}^{(X)} \tilde{\mathcal{X}}_{o,L}^{(X)} \tilde{\mathcal{X}}_{o,R}^{(X)} \\ (v_c, v_2) \quad (v_c, v_3) \end{matrix} \begin{matrix} \tilde{\mathcal{X}}_{e,L}^{(X)} \tilde{\mathcal{X}}_{e,R}^{(Z)} \\ (v_c, N(v_c) \setminus \{v_2, v_3\}) \end{matrix} \mathcal{S}_{v_2} \mathcal{S}_{v_3} \quad (\text{C23})$$

$$\cdot \tilde{\mathcal{X}}_{v_c} \mathcal{X}_{v_1} \mathcal{Z}_{v_2} \mathcal{X}_{v_3} \mathcal{Z}^{N(v_c) \setminus V_3} \begin{matrix} \tilde{\mathcal{X}}_{o,L}^{(X)} \tilde{\mathcal{X}}_{o,R}^{(X)} \\ (v_c, v_1) \end{matrix} \begin{matrix} \tilde{\mathcal{X}}_{o,L}^{(X)} \tilde{\mathcal{X}}_{o,R}^{(X)} \\ (v_c, v_3) \end{matrix} \begin{matrix} \tilde{\mathcal{X}}_{e,L}^{(X)} \tilde{\mathcal{X}}_{e,R}^{(Z)} \\ (v_c, N(v_c) \setminus \{v_1, v_3\}) \end{matrix} \mathcal{S}_{v_1} \mathcal{S}_{v_3} | \Psi \rangle \quad (\text{C24})$$

$$= (-1) \mathcal{Z}_{v_1} \mathcal{X}_{v_1} \mathcal{Z}_{v_1} \mathcal{X}_{v_1} | \Psi \rangle. \quad (\text{C25})$$

Line (C22) was obtained by using Eqs. (C19)-(C6). The following four lines, constituting Eq. (C23) are obtained by using Eq. (B10) and Eq. (B12). Line (C24) was obtained by using that the physical measurement observables square to the identity, so that we are only left with observables on the power vertex v_1 . We obtained the anti-commutation relation between observables on the power vertex v_1 .

A simple visualization of the calculus a circle with three vertices v_1, v_2, v_3 is an array whose rows contain the measurements and the deterministic outcome, which was given in the main text.

If the physical experiment (PE) simulates the reference experiment (RE) 2 for $N(v_c) = \{v_1, v_2\}$ such that $|N(v_c)| = 2$, the specified correlations from the measurements fulfill

$$\langle \Psi | \zeta_u | \Psi \rangle = 1, \quad \forall u \in V, \quad (\text{C26})$$

$$\langle \Psi | \tilde{\zeta}_{v_c} | \Psi \rangle = 1, \quad (\text{C27})$$

$$\langle \Psi | \mathcal{C}_{v_c} | \Psi \rangle = -1, \quad (\text{C28})$$

$$\langle \Psi | \mathcal{C}_{v_1} | \Psi \rangle = 1, \quad (\text{C29})$$

$$\langle \Psi | \mathcal{C}_{v_2} | \Psi \rangle = 1, \quad (\text{C30})$$

$$\langle \Psi | \mathcal{C}_2^{(X)} | \Psi \rangle = 1. \quad (\text{C31})$$

$$\langle \Psi | \mathcal{C}_2^{(Y)} | \Psi \rangle = 1. \quad (\text{C32})$$

Since the norm of all physical measurement observables is at most 1, Eqs. (C26)-(C32) imply

$$\zeta_u |\Psi\rangle = |\Psi\rangle, \quad \forall u \in V, \quad (\text{C33})$$

$$\tilde{\zeta}_{v_c} |\Psi\rangle = |\Psi\rangle, \quad (\text{C34})$$

$$(-1)\mathcal{C}_{v_c} |\Psi\rangle = |\Psi\rangle, \quad (\text{C35})$$

$$\mathcal{C}_{v_1} |\Psi\rangle = |\Psi\rangle, \quad (\text{C36})$$

$$\mathcal{C}_{v_2} |\Psi\rangle = |\Psi\rangle, \quad (\text{C37})$$

$$\mathcal{C}_2^{(X)} |\Psi\rangle = |\Psi\rangle. \quad (\text{C38})$$

$$\mathcal{C}_2^{(Y)} |\Psi\rangle = |\Psi\rangle. \quad (\text{C39})$$

Recall that any vertex's observable depends on the measurement observables from all vertices $v \in N_d(u)$. As explained in the main text, whenever a vertex is not asked to measure anything in the RE, in the PE it is given an input, but the results are marginalized. Thus, physical measurement \mathcal{C}_v has two non-equivalent implementations, one in which the vertex which does not measure anything in the RE is asked to perform the measurement corresponding to X and the other in which it is asked to measure Z . We write $\mathcal{C}_2^{(X)}$ and $\mathcal{C}_2^{(Y)}$ for these two physical implementations, respectively. Both operators have congruent observables except on the chain vertices with the nearest power vertex v_c , thus

$$\mathcal{C}_{v_c}^{(Y)} \mathcal{C}_{v_c}^{(X)} = \tilde{\mathcal{X}}_{o,L}^{(Y)} \tilde{\mathcal{X}}_{e,L}^{(X)} \underset{(v_c, N(v_c))}{.} \quad (\text{C40})$$

Then, we get the following chain of relations

$$|\Psi\rangle = (-1)\mathcal{C}_{v_c} \tilde{\zeta}_{v_c} \mathcal{C}_{v_1} \mathcal{C}_{v_2} \mathcal{C}_2^{(Y)} \mathcal{C}_2^{(X)} |\Psi\rangle \quad (\text{C41})$$

$$\begin{aligned} &= (-1) \tilde{\mathcal{X}}_{v_c} \mathcal{X}_{v_1} \mathcal{X}_{v_2} \tilde{\mathcal{X}}_{o,L}^{(X)} \tilde{\mathcal{X}}_{o,R}^{(X)} \tilde{\mathcal{X}}_{o,L}^{(X)} \tilde{\mathcal{X}}_{o,R}^{(X)} \mathcal{S}_{v_1} \mathcal{S}_{v_2} \\ &\quad \cdot \tilde{\mathcal{X}}_{v_c} \mathcal{Z}_{v_1} \mathcal{Z}_{v_2} \tilde{\mathcal{X}}_{e,L}^{(X)} \tilde{\mathcal{X}}_{e,R}^{(Z)} \tilde{\mathcal{X}}_{e,L}^{(X)} \tilde{\mathcal{X}}_{e,R}^{(Z)} \underset{(v_c, v_2)}{.} \\ &\quad \cdot \tilde{\mathcal{Y}}_{v_c} \mathcal{X}_{v_1} \mathcal{Z}_{v_2} \tilde{\mathcal{X}}_{o,L}^{(Y)} \tilde{\mathcal{X}}_{o,R}^{(X)} \tilde{\mathcal{X}}_{e,L}^{(Y)} \tilde{\mathcal{X}}_{e,R}^{(Z)} \mathcal{S}_{v_1} \underset{(v_c, v_2)}{.} \\ &\quad \cdot \tilde{\mathcal{Y}}_{v_c} \mathcal{Z}_{v_1} \mathcal{X}_{v_2} \tilde{\mathcal{X}}_{e,L}^{(Y)} \tilde{\mathcal{X}}_{e,R}^{(Z)} \tilde{\mathcal{X}}_{o,L}^{(Y)} \tilde{\mathcal{X}}_{o,R}^{(X)} \mathcal{S}_{v_2} \underset{(v_c, v_2)}{.} \\ &\quad \cdot \tilde{\mathcal{X}}_{o,L}^{(Y)} \tilde{\mathcal{X}}_{e,L}^{(X)} \tilde{\mathcal{X}}_{o,L}^{(Y)} \tilde{\mathcal{X}}_{e,L}^{(X)} \underset{(v_c, v_1)}{.} \end{aligned} \quad (\text{C42})$$

$$= (-1)\mathcal{Z}_{v_1} \mathcal{X}_{v_1} \mathcal{Z}_{v_1} \mathcal{X}_{v_1} |\Psi\rangle. \quad (\text{C43})$$

Line (C41) was obtained by using Eqs. (C33)-(C39). The following five lines, constituting Eq. (C42) are obtained by using Eqs. (B2), (B17)-(B21), and Eq. (C40). Taking that the physical measurement observables square to the identity gives line (C43). We obtained the anti-commutation relation between observables on the power vertex v_1 .

The same anti-commutation relation for all other power vertices follows from Lemma 2. \square

Proof [Lemma 1, Reference experiment 3.] If the physical experiment (PE) simulates the reference experiment (RE) 3, the specified correlations from the measurements fulfill

$$\langle \Psi | \zeta_u | \Psi \rangle = 1, \quad \forall u \in V, \quad (\text{C44})$$

$$\langle \Psi | \mathcal{I}_1 | \Psi \rangle = (-1)^{d+1} \frac{1}{\sqrt{2}}, \quad (\text{C45})$$

$$\langle \Psi | \mathcal{I}_2 | \Psi \rangle = (-1)^d \frac{1}{\sqrt{2}}, \quad (\text{C46})$$

$$\langle \Psi | \mathcal{I}_3 | \Psi \rangle = \frac{1}{\sqrt{2}}, \quad (\text{C47})$$

$$\langle \Psi | \mathcal{I}_4 | \Psi \rangle = \frac{1}{\sqrt{2}}, \quad (\text{C48})$$

$$\langle \Psi | \mathcal{P}_1 | \Psi \rangle = 1. \quad (\text{C49})$$

$$\langle \Psi | \mathcal{P}_2 | \Psi \rangle = 1. \quad (\text{C50})$$

Then, it follows from Eqs. (C45)-(C48) that

$$\langle \Psi | \left(2\sqrt{2}\mathbb{1} + (-1)^d(\mathcal{I}_1 - \mathcal{I}_2) - \mathcal{I}_3 - \mathcal{I}_4 \right) | \Psi \rangle = 0. \quad (\text{C51})$$

The operator has at least three decompositions into sums of squares

$$\begin{aligned} 4\mathbb{1} + \sqrt{2}((-1)^d(\mathcal{I}_1 - \mathcal{I}_2) - \mathcal{I}_3 - \mathcal{I}_4) &= \left[\sqrt{2}\mathbb{1} + \frac{1}{2}((-1)^d(\mathcal{I}_1 - \mathcal{I}_2) - \mathcal{I}_3 - \mathcal{I}_4) \right]^2 + \left[\frac{1}{2}((-1)^d(\mathcal{I}_1 + \mathcal{I}_2) - \mathcal{I}_3 + \mathcal{I}_4) \right]^2 \\ &= \left[\mathcal{A}_0 - \frac{\mathcal{B}_0 - (-1)^d\mathcal{B}_1}{\sqrt{2}} \right]^2 + \left[\mathcal{A}_1 - \frac{\mathcal{B}_1 + (-1)^d\mathcal{B}_0}{\sqrt{2}} \right]^2 \end{aligned} \quad (\text{C52})$$

$$= \left[\mathcal{B}_0 - \frac{\mathcal{A}_0 - (-1)^d\mathcal{A}_1}{\sqrt{2}} \right]^2 + \left[\mathcal{B}_1 - \frac{\mathcal{A}_1 + (-1)^d\mathcal{A}_0}{\sqrt{2}} \right]^2. \quad (\text{C53})$$

with $\mathcal{I}_1 = \mathcal{A}_0 \mathcal{B}_1$, $\mathcal{I}_2 = \mathcal{A}_1 \mathcal{B}_0$, $\mathcal{I}_3 = \mathcal{A}_1 \mathcal{B}_1$, $\mathcal{I}_4 = \mathcal{A}_0 \mathcal{B}_0$, and, using Eqs. (B28)-(B31),

$$\mathcal{A}_0 := \tilde{\mathcal{Z}}_{v_l}^{(R)} \tilde{\mathcal{X}}_{o,L}^{(Z,R)} \mathcal{R}_{d(v_l, v_r)}^{(Z)}, \quad \mathcal{A}_1 := S_{v_l} \tilde{\mathcal{O}}_{v_l}^{(R)} \tilde{\mathcal{X}}_{e,L}^{(O,R)} \mathcal{R}_{d(v_l, v_r)}^{(O)}, \quad \mathcal{B}_0 := \tilde{\mathcal{X}}_{e,R}^{(Z,R)} \tilde{\mathcal{Z}}_{v_r}, \quad \mathcal{B}_1 := \tilde{\mathcal{X}}_{o,R}^{(X,R)} \tilde{\mathcal{X}}_{v_r} S_{v_r}.$$

The first decomposition holds since $\mathcal{I}_1 \mathcal{I}_4 = \mathcal{I}_3 \mathcal{I}_2 = \mathcal{B}_1 \mathcal{B}_0$ and $\mathcal{I}_4 \mathcal{I}_1 = \mathcal{I}_2 \mathcal{I}_3 = \mathcal{B}_0 \mathcal{B}_1$. From Eq. (C51) it is

$$\begin{aligned} 2\sqrt{2}\mathbb{1} + (-1)^d(\mathcal{I}_1 - \mathcal{I}_2) - \mathcal{I}_3 - \mathcal{I}_4 | \Psi \rangle &= 0, & (-1)^d(\mathcal{I}_1 + \mathcal{I}_2) - \mathcal{I}_3 + \mathcal{I}_4 | \Psi \rangle &= 0, \\ \left[\mathcal{A}_0 - \frac{\mathcal{B}_0 - (-1)^d\mathcal{B}_1}{\sqrt{2}} \right] | \Psi \rangle &= 0, & \left[\mathcal{A}_1 - \frac{\mathcal{B}_1 + (-1)^d\mathcal{B}_0}{\sqrt{2}} \right] | \Psi \rangle &= 0, \\ \left[\mathcal{B}_0 - \frac{\mathcal{A}_0 - (-1)^d\mathcal{A}_1}{\sqrt{2}} \right] | \Psi \rangle &= 0, & \left[\mathcal{B}_1 - \frac{\mathcal{A}_1 + (-1)^d\mathcal{A}_0}{\sqrt{2}} \right] | \Psi \rangle &= 0. \end{aligned}$$

Then, one can write

$$\mathcal{A}_0 \mathcal{A}_1 + \mathcal{A}_0 \mathcal{A}_1 = \mathcal{A}_0 \left[\mathcal{A}_1 - \frac{\mathcal{B}_1 + (-1)^d\mathcal{B}_0}{\sqrt{2}} \right] + \mathcal{A}_1 \left[\mathcal{A}_0 - \frac{\mathcal{B}_0 - (-1)^d\mathcal{B}_1}{\sqrt{2}} \right] + \frac{(-1)^d [(-1)^d(\mathcal{I}_1 + \mathcal{I}_2) - \mathcal{I}_3 + \mathcal{I}_4]}{\sqrt{2}}, \quad (\text{C54})$$

$$\mathcal{B}_0 \mathcal{B}_1 + \mathcal{B}_0 \mathcal{B}_1 = \mathcal{B}_0 \left[\mathcal{B}_1 - \frac{\mathcal{A}_1 + (-1)^d\mathcal{A}_0}{\sqrt{2}} \right] + \mathcal{B}_1 \left[\mathcal{B}_0 - \frac{\mathcal{A}_0 - (-1)^d\mathcal{A}_1}{\sqrt{2}} \right] + \frac{(-1)^d [(-1)^d(\mathcal{I}_1 + \mathcal{I}_2) - \mathcal{I}_3 + \mathcal{I}_4]}{\sqrt{2}} \quad (\text{C55})$$

As a result, we obtain

$$\mathcal{A}_0 \mathcal{A}_1 + \mathcal{A}_0 \mathcal{A}_1 | \Psi \rangle = 0, \quad \mathcal{B}_0 \mathcal{B}_1 + \mathcal{B}_0 \mathcal{B}_1 | \Psi \rangle = 0,$$

which imply the anti-commutation relations

$$\{\tilde{\mathcal{O}}_{v_l} \mathcal{R}_{d(v_l, v_r)}^{(O)}, \tilde{\mathcal{Z}}_{v_l} \mathcal{R}_{d(v_l, v_r)}^{(Z)}\} | \Psi \rangle = 0, \quad \{\tilde{\mathcal{X}}_{v_r}, \tilde{\mathcal{Z}}_{v_r}\} | \Psi \rangle = 0,$$

respectively. Furthermore, we can obtain the anti-commutation relation $\{\mathcal{O}_{v_l} \mathcal{X}_{d(v_l, v_r)}^{(O)}, \mathcal{Z}_{v_l} \mathcal{X}_{d(v_l, v_r)}^{(Z)}\} | \Psi \rangle = 0$ from the previous and $\mathcal{P}_1 \mathcal{P}_2 \mathcal{P}_1 \mathcal{P}_2 | \Psi \rangle = | \Psi \rangle$.

Together with the above anti-commutation relations, we obtain $\{\mathcal{X}_v, \mathcal{Z}_v\} | \Psi \rangle = 0$ from

$$\zeta_v \mathcal{P}_2 \zeta_v \mathcal{P}_2 | \Psi \rangle = | \Psi \rangle, \quad \text{for } v \in N(v_l), \quad \zeta_v \mathcal{P}_1 \zeta_v \mathcal{P}_1 | \Psi \rangle = | \Psi \rangle, \quad \text{for } v \in N(v_r). \quad (\text{C56})$$

All other anti-commutation relations follow from Lemma 2. \square

Lemma 2. Consider a physical experiment with the state $| \Psi \rangle$ and correlations

$$\zeta_u = \mathcal{X}_u \tilde{\mathcal{X}}_{e,L}^{(X)} \tilde{\mathcal{X}}_{o,R}^{(Z)} \tilde{\mathcal{Z}}^{N(u)}, \quad (\text{C57})$$

$$\tilde{\zeta}_v = \tilde{\mathcal{X}}_v \tilde{\mathcal{X}}_{e,L}^{(X)} \tilde{\mathcal{X}}_{o,R}^{(Z)} \mathcal{Z}^{N(v)}, \quad (\text{C58})$$

such that

$$\langle \Psi | \zeta_u | \Psi \rangle = \langle \Psi | \tilde{\zeta}_v | \Psi \rangle = 1, \quad (\text{C59})$$

for $u \in N(v)$, $v \in N(u)$.

If $\{\mathcal{X}_u, \mathcal{Z}_u\} | \Psi \rangle = 0$, then it also holds that $\{\tilde{\mathcal{X}}_v, \tilde{\mathcal{Z}}_v\} | \Psi \rangle = 0$.

Note that in most applications of Lemma 2, $\tilde{\zeta}_v = \zeta_v$. In general, the correlations $\zeta_v, \tilde{\zeta}_v$ can stem from different measurements, if the difference is not apparent on the marginalized observables. In particular, it suffices that the marginalized observables do not overlap but on the power vertices that are of interest for the anti-commutation relation.

Proof. Given the requirements, it is $\zeta_u|\Psi\rangle = \zeta_v|\Psi\rangle = |\Psi\rangle$ and $\mathcal{Z}_u\mathcal{X}_u\mathcal{Z}_u\mathcal{X}_u|\Psi\rangle = (-1)|\Psi\rangle$. Then, we evaluate

$$|\Psi\rangle = \tilde{\zeta}_v\zeta_u\tilde{\zeta}_v\zeta_u|\Psi\rangle = (\mathcal{Z}_u\mathcal{X}_u\mathcal{Z}_u\mathcal{X}_u)(\tilde{\mathcal{X}}_v\tilde{\mathcal{Z}}_v\tilde{\mathcal{X}}_v\tilde{\mathcal{Z}}_v)|\Psi\rangle = (-1)\tilde{\mathcal{X}}_v\tilde{\mathcal{Z}}_v\tilde{\mathcal{X}}_v\tilde{\mathcal{Z}}_v|\Psi\rangle.$$

We use Eq. (C57) and Eq. (C58), and that the observables of the physical measurement square to identity. It follows that $\{\tilde{\mathcal{X}}_v, \tilde{\mathcal{Z}}_v\}|\Psi\rangle = 0$. \square

Appendix D: Self-testing symmetric graph states against communication

For the standard self-testing proof, we require observable of the physical experiment to reproduce the graph's stabilizer conditions, specifically that of the generator elements, and anti-commutation relations for observables that are involved in the products of observables that reproduce these conditions, specifically corresponding to the Pauli X and Z observables. In a scenario with bounded classical communication, The local observable corresponding to the Pauli X operator must also include the information that its nearest neighbors measure in the Pauli Z basis, and vice versa.

We present the proof for the ideal case $\epsilon = \delta = 0$. For a robust version of the equivalence, we refer to the one of RE 1 and RE 2 in Tab. I.

Proof. [$\epsilon = \delta = 0$] Given a physical experiment with state $|\Psi\rangle$ and measurement observables that are compatible and simulates the RE 4. The RE include RE 1 such that Lemma 1 applies, i.e. $\{\mathcal{X}_u, \mathcal{Z}_u\}|\Psi\rangle = 0$ for all $u \in V'$. The observables rely on the vertices within communication distance d to perform measurements in the Pauli X basis.

We denote the tensor product of observables $\tilde{\zeta}_u^{(X)}$ and $\tilde{\zeta}_u^{(Z)}$ correspond to the Pauli submeasurements f_u of the measurements $\tilde{M}_u^{(X)}$ in Eq. (20) and $\tilde{M}_u^{(Z)}$ in Eq. (21), respectively. From the simulation condition,

$$\langle\Psi|\tilde{\zeta}_u^{(X)}|\Psi\rangle = \langle\Psi|\tilde{\zeta}_u^{(Z)}|\Psi\rangle = 1, \quad (\text{D1})$$

and, therefore, $\tilde{\zeta}_u^{(X)}|\Psi\rangle = \tilde{\zeta}_u^{(Z)}|\Psi\rangle = |\Psi\rangle$ for all $u \in V'$.

We evaluate $\tilde{\zeta}_u^{(X)}\tilde{\zeta}_v^{(Z)}\tilde{\zeta}_u^{(X)}\tilde{\zeta}_v^{(Z)}|\Psi\rangle = |\Psi\rangle$ for any two neighboring vertices with distance $\text{dist}(u, v) = 2d + 1$. Namely, we multiply the local observables column wise

$$\begin{aligned} \zeta_u^{(X)} &= \mathcal{X}_u & \tilde{\mathcal{X}}_{e,L}^{(X)} & & \tilde{\mathcal{X}}_{e,R}^{(Z)} & Z_v \\ & & (u,v) & & (u,v) & \\ \zeta_v^{(Z)} &= \mathcal{Z}_u & \tilde{\mathcal{X}}_{o,L}^{(Z)} & & \tilde{\mathcal{X}}_{o,R}^{(X)} & X_v, \\ & & (u,v) & & (u,v) & \\ \zeta_u^{(X)} &= \mathcal{X}_u & \tilde{\mathcal{X}}_{o,L}^{(X)} & & \tilde{\mathcal{X}}_{o,R}^{(Z)} & Z_v \\ & & (u,v) & & (u,v) & \\ \zeta_v^{(Z)} &= \mathcal{Z}_u & \tilde{\mathcal{X}}_{o,L}^{(Z)} & & \tilde{\mathcal{X}}_{o,R}^{(X)} & X_v, \\ & & (u,v) & & (u,v) & \end{aligned} \quad (\text{D2})$$

similar to Lemma 2, where X_v, Z_v are observables whose neighboring vertices up to distance d measure the observables X and Z in an alternating pattern. As a result, we obtain Eq. (27)

$$\{X_v, Z_v\}|\Psi\rangle = 0 \quad (\text{D3})$$

from $\{\mathcal{X}_u, \mathcal{Z}_u\}|\Psi\rangle = 0$. The submeasurements g_u from settings corresponding to $M_u^{(alt)}$ in Eq. (24) lead to Eq. (28) for the product of observables ξ_u ,

$$\xi_u|\Psi\rangle = X_u \bigotimes_{v \in N(u)} Z_v|\Psi\rangle = |\Psi\rangle. \quad (\text{D4})$$

As a result, the physical state reproduces the stabilizer conditions of the inflated circular graph state.

Given a physical experiment with state $|\Psi\rangle$ and measurement observables that are compatible and simulates the RE 5. The RE contain RE 2 for a tripoint star graph around vertex v_c in the honeycomb lattice, such that Lemma 1

applies with an anti-commutation relation $\{\mathcal{X}_u, \mathcal{Z}_u\}|\Psi\rangle = 0$ for the power vertices of the inflated star graph v_c and $v \in N'(v_c)$, which are the vertices in the corners of the tripoint star. However, these observables rely on the vertices on the tripoint star within communication distance d to perform measurements in the Pauli X basis.

We denote the tensor product of observables $\tilde{\zeta}_{v_0}^{(X)}$ corresponds to the submeasurement f_{v_0} from measurements $\tilde{M}_{v_0}^{(X)}$ in Eq. (22), and $\tilde{\zeta}_{v_c}^{(Z)}$ corresponds to f_{v_c} from $\tilde{M}_{v_0}^{(Z)}$ in Eq. (23). Additionally, the tensor product of observables $\tilde{\zeta}_u^{(alt)}$ corresponds to the submeasurement f_u from measurements $M_1^{(alt)}$ in Eq. (25) if $u \in V_{hex_1}$ or from $M_2^{(alt)}$ in Eq. (26) if $u \in V_{hex_2}$. From the simulation condition,

$$\langle \Psi | \tilde{\zeta}_{v_0}^{(X)} | \Psi \rangle = \langle \Psi | \tilde{\zeta}_{v_c}^{(Z)} | \Psi \rangle = \langle \Psi | \tilde{\zeta}_u^{(alt)} | \Psi \rangle = 1, \quad (D5)$$

and, therefore, $\tilde{\zeta}_{v_0}^{(X)}|\Psi\rangle = \tilde{\zeta}_{v_c}^{(Z)}|\Psi\rangle = \tilde{\zeta}_u^{(alt)}|\Psi\rangle = |\Psi\rangle$.

First, we evaluate $\zeta_{v_0}^{(X)}\zeta_{v_c}^{(Z)}\zeta_{v_0}^{(X)}\zeta_{v_c}^{(Z)}|\Psi\rangle = |\Psi\rangle$ for any two neighboring vertices with distance $dist(u, v) = 2d + 1$ in the same way as in the proof of Lemma 2. As a result, $\{\mathcal{X}_{v_c}, \mathcal{Z}_{v_c}\}|\Psi\rangle = 0$ from $\{\mathcal{X}_{v_0}, \mathcal{Z}_{v_0}\}|\Psi\rangle = 0$, for observables X, Z that correspond to measurement settings where the neighboring vertices up to distance d measure the observables X and Z in an alternating pattern.

We propagate the anti-commutation relation (D3) to every vertex of the honeycomb lattice starting with v_c and consecutively evaluating $\tilde{\zeta}_u^{(alt)}\tilde{\zeta}_v^{(alt)}\tilde{\zeta}_u^{(alt)}\tilde{\zeta}_v^{(alt)}|\Psi\rangle = |\Psi\rangle$ in the same way as in the proof of Lemma 2. The vertex u is at the center of a tripoint star and vertex v at distance $dist(u, v) = 2d + 1$ in one of the corners of the tripoint star. Then, it is $\{\mathcal{X}_v, \mathcal{Z}_v\}|\Psi\rangle = 0$ from $\{\mathcal{X}_u, \mathcal{Z}_u\}|\Psi\rangle = 0$. The submeasurements g_u from settings corresponding to $M_{hex_1}^{(alt)}$ in Eq. (25) if $u \in V_{hex_1}$ or $M_{hex_2}^{(alt)}$ in Eq. (26) if $u \in V_{hex_2}$ lead to Eq. (28) for the product of observables ξ_u ,

$$\xi_u|\Psi\rangle = \mathcal{X}_u \bigotimes_{v \in N(u)} \mathcal{Z}_v|\Psi\rangle = |\Psi\rangle. \quad (D6)$$

As a result, the physical state reproduces the stabilizer conditions of the inflated circular graph state.

We show the equivalence in terms of Def. 3 between the PE and the RE with the local isometry is $\Phi = \prod_{v \in V'(V_{hex})} \phi_v$ with ϕ_v characterized by the first circuit in Fig. 1 using the observables \mathcal{X}_u and \mathcal{Z}_u . The evaluation of the isometry is the same as in Appendix A, but we use $\xi_u|\Psi\rangle = \mathcal{X}_u(\mathcal{Z}^{N(u)}|\Psi\rangle = |\Psi\rangle$ and the anti-commutation relation in Eq. (D3). The tensor product of observables ξ_u corresponds to the measurement submeasurements g_u from $M_u^{(X)}$ for RE 4 and from $M^{(alt)}$ for RE 5. \square

Appendix E: Inflated Isomorphism

Here, we proof Theorem 1 for the ideal case, $\epsilon = 0$ and $\delta = 0$. In Appendix F, we extend the proof to robust equivalence by trailing the proof for the ideal case and bounding all expressions that result from the accordance of the measurement correlations.

Consider a physical experiment (PE) that is compatible and simulate one of the reference experiments (REs) 1,2 and 3, such that Lemma 1 applies, and it is $\zeta_u|\Psi\rangle = |\Psi\rangle$ for all $u \in V$.

Measuring the chain vertices in the measurement bases corresponding to observable \mathcal{X} with outcome $\mathbf{x} = (x_v)_{v \in V' \setminus V}$, transforms the state

$$|\Psi\rangle \longrightarrow |\Psi'\rangle = \Pi_{\mathcal{X}}^{(\mathbf{x})}|\Psi\rangle = \bigotimes_{v \in V' \setminus V} (\mathbb{1}_v + (-1)^{x_v} \mathcal{X}_v) |\Psi\rangle. \quad (E1)$$

The isometry that maps the subsequent state (on the power vertices) to the graph state corresponding to the graph in the RE is a product of local isometries for each power vertex. The local isometries are described by the first circuit in Fig. 1. We employ the standard isometry inspired on the SWAP gate in Fig. 1, which was proposed in [10], used in [42] and in Section A.

The isometry acts locally on the post-measurement state and one ancilla qubit for every power vertex,

$$\Phi \left(|\mathbf{0}\rangle \otimes \Pi_{\mathcal{X}}^{(\mathbf{x})}|\Psi\rangle \right) = \prod_{v \in V} \phi_v \left(|\mathbf{0}\rangle \otimes \Pi_{\mathcal{X}}^{(\mathbf{x})}|\Psi\rangle \right). \quad (E2)$$

$(x_e)_v := \sum_{s=1}^d x_{2s(v, N(v))}$, *i.e.* the sum of measurement outcomes of every second chain vertex seen from the power

vertex v up to the next power vertices. Denoting $Z_{\mathbf{a}}^{\mathbf{x}_e} = \bigotimes_{u \in V} Z_{a_u}^{(x_e)_u}$, it is

$$\Phi \left(|0\rangle \otimes \Pi_{\mathcal{X}}^{(\mathbf{x})} |\Psi\rangle \right) = \frac{1}{2^{|V|}} \sum_{\mathbf{a} \in \mathbb{F}_2^{|V|}} |\mathbf{a}\rangle \otimes \Pi_{\mathcal{X}}^{(\mathbf{x})} \bigotimes_{u \in V} (\mathbb{1}_u + \mathcal{Z}_u) \mathcal{X}_u^{a_u} |\Psi\rangle \quad (\text{E3})$$

$$= \frac{1}{2^{|V|}} \sum_{\mathbf{a} \in \mathbb{F}_2^{|V|}} (-1)^{g(\mathbf{a})} |\mathbf{a}\rangle \otimes \Pi_{\mathcal{X}}^{(\mathbf{x})} \bigotimes_{u \in V} \left(\mathcal{X}_{e,L}^{(X)} \mathcal{X}_{e,R}^{(Z)} \right)_{(u, N(u))}^{a_u} (\mathbb{1}_u + \mathcal{Z}_u) |\Psi\rangle \quad (\text{E4})$$

$$= \frac{1}{2^{|V|}} \sum_{\mathbf{a} \in \mathbb{F}_2^{|V|}} (-1)^{g(\mathbf{a}) + \mathbf{x}_e \cdot \mathbf{a}} |\mathbf{a}\rangle \otimes \Pi_{\mathcal{X}}^{(\mathbf{x})} \bigotimes_{u \in V} (\mathbb{1}_u + \mathcal{Z}_u) |\Psi\rangle \quad (\text{E5})$$

$$= |G^{(\mathbf{x})}\rangle \otimes |junk\rangle, \quad (\text{E6})$$

with the graph state's signature

$$g(\mathbf{a}) := \sum_{(u,v) \in E} a_u a_v.$$

Line (E3) was obtained by evaluating the action of the circuit ϕ_v , which has been done in Eq.(A1) in Appendix A.

To arrive at Eq.(E4), consider an arbitrary but fixed order of vertices and sequentially perform the following three steps. First, from $\zeta_u |\Psi\rangle = |\Psi\rangle$ and Eq.(B2), apply

$$\mathcal{X}_u^{a_u} |\Psi\rangle = \left(\left(\mathcal{X}_{e,L}^{(X)} \mathcal{X}_{e,R}^{(Z)} \right) Z^{N(u)} \right)_{(u, N(u))}^{a_u} |\Psi\rangle.$$

With the anti-commutations relations, permute $Z^{N(u)}$ from right to left. Depending on the order of vertices, if $u < v \in N(u)$, $(\mathcal{Z}_v)^{a_v}$ anti-commutes with $(\mathcal{X}_v)^{a_v}$, leading to a phase $(-1)^{a_u a_v}$ which is acquired if and only if two vertices share an edge. Then, absorb $(\mathbb{1}_u + \mathcal{Z}_u) (\mathcal{Z}_v)^{a_v} = (\mathbb{1}_u + \mathcal{Z}_u)$.

For Eq.(E5), use $\Pi_{\mathcal{X}}^{(\mathbf{x})} \mathcal{X} = (-1)^x \Pi_{\mathcal{X}}^{(\mathbf{x})}$ for the operators on the chain vertices. To arrive at Eq.(E6), define the locally rotated graph state

$$|G^{(\mathbf{x})}\rangle = \frac{1}{2^{|V|/2}} \sum_{\mathbf{a} \in \mathbb{F}_2^{|V|}} (-1)^{g(\mathbf{a}) + \mathbf{x}_e \cdot \mathbf{a}} |\mathbf{a}\rangle, \quad (\text{E7})$$

and a residual state

$$|junk\rangle = 2^{|V|/2} \Pi_{\mathcal{X}}^{(\mathbf{x})} \bigotimes_{u \in V} (\mathbb{1}_u + \mathcal{Z}_u) |\Psi\rangle. \quad (\text{E8})$$

There are three caveats regarding RE 3. First, for odd d , the correction operation $Z_{a_{v_l}}^{(x_e)_{v_l}}$ on vertex v_l depends additionally on the measurement outcomes of chain vertex $d_{(v_l, v_r)}$, *i.e.* $(x_e)_{v_l} \rightarrow (x_e)_{v_l} + x_{d_{(v_l, v_r)}}$. Second, $\mathcal{X}_{v_l} \mathcal{Z}_{v_l} |\Psi\rangle = (-1) \mathcal{Q} \mathcal{Z}_{v_l} \mathcal{X}_{v_l} |\Psi\rangle$ with $\mathcal{Q} := (\mathcal{X}^{(Z)} \mathcal{X}^{(O)} \mathcal{X}^{(Z)} \mathcal{X}^{(O)})_{d_{(v_l, v_r)}}$. Throughout the above considerations, \mathcal{Q} occurs whenever one uses the anti-commutation relation. However, it can immediately be absorbed in the measurement projectors since $\Pi_{\mathcal{X}}^{(\mathbf{x})} \mathcal{Q} = \Pi_{\mathcal{X}}^{(\mathbf{x})}$ and therefore does not affect the result. Third, for $d = 1$, we replace the observable \mathcal{X}_{v_l} by \mathcal{Y}_{v_l} in the isomorphism.

For any measurement of the PE \mathcal{M}_k , the action under the isometry is $\Phi^{(\mathbf{x})} \left(|0\rangle \otimes \Pi_{\mathcal{X}}^{(\mathbf{x})} \mathcal{M}_k |\Psi\rangle \right)$. Since all measurements can be composed into products of observables \mathcal{Z} and \mathcal{X} on the power vertices and operators \mathcal{X} on the chain vertices, we consider these separately. For some power vertex v and $\Phi^{(\mathbf{x})} \left(|0\rangle \otimes \Pi_{\mathcal{X}}^{(\mathbf{x})} \mathcal{X}_v |\Psi'\rangle \right)$, insert X_v to the right of Eq.(E3) to see that it shifts $a_v \rightarrow (a_v + 1) \bmod 2$. This is exactly the action of a Pauli X operator on $|a_v\rangle$. For $\Phi^{(\mathbf{x})} \left(|0\rangle \otimes \Pi_{\mathcal{X}}^{(\mathbf{x})} \mathcal{Z}_v |\Psi'\rangle \right)$, inserting Z_v to the right of Eq.(E3), and anti-commute it with $\mathcal{X}_v^{a_v}$ for a sign factor $(-1)^{a_v}$, which is exactly the action of a Pauli Z operator on $|a_v\rangle$. For any chain vertex v , $\Pi_{\mathcal{X}}^{(\mathbf{x})} \mathcal{X}_v = (-1)^{x_v} \Pi_{\mathcal{X}}^{(\mathbf{x})}$ leads to a global phase, undetectable by any measurement. By linearity, it is then $\Phi^{(\mathbf{x})} \left(|0\rangle \otimes \Pi_{\mathcal{X}}^{(\mathbf{x})} \mathcal{M}_k |\Psi\rangle \right) = M_k |G\rangle \otimes |junk\rangle$, for any measurement setting M_k reduced to its action on the power vertices. This concludes our proof of Theorem 1.

In Appendix F, we extend Theorem 1 to a robust self-testing procedure with techniques present in [42] and in [50]. The bounds on the isometry for all discussed REs are in Tab.I. They scale with $\sqrt{\epsilon}$ where ϵ is the deviation of the measurement results from the ideal ones, as in Def. 4. The bounds on the self-testing procedure with inflated graph states allowing bounded classical communication are slightly worse than for the non-inflated graph states, which is mainly due to the higher number of measurements required to derive the anti-commutation relations.

Reference experiment	c	Robustness
RE 6	4	$\delta = \sqrt{\epsilon} V (2 V ^2 + 6 V + 6)$
RE 1	$3m + 1$	$\delta = \sqrt{\epsilon} V (\frac{7}{2} V ^2 + \frac{15}{2} V + 2)$
RE 2		
$ N(v_c) = 2$	6	$\delta = \sqrt{\epsilon} V (2 V ^2 + 7 V + 8)$
$ N(v_c) > 2$	$4 + 4 N(v_c) $	$\delta = \sqrt{\epsilon} V (2 V ^2 + 6 V + 6)$
RE 3	$\sqrt{8\sqrt{2}}(1 + \sqrt{2})$	$\delta = \sqrt{\epsilon} V [2 V ^2 + 4 V + 1 + (2 + V)\sqrt{2\sqrt{2}}(1 + \sqrt{2})]$
Def. 3 in [42]	$m + 1$	$\delta = \sqrt{\epsilon} V (\frac{5}{2} V ^2 + \frac{11}{2} V + 2)$
Def. 4 in [42]	–	$\delta = \sqrt{\epsilon} V (2 V ^2 + 4 V + 1) + V \sqrt[4]{\epsilon} (\frac{13}{2} V + 13)$

TABLE I: Table of bounds on robustness δ in Def. 4 from Eq. (F3), parameter c , with $|E| \leq |V|^2$ and $l \leq |V|$. Note that m is the number of vertices in the circle in RE 1.

Appendix F: Self-testing robustness

We show that our self-testing proofs from Theorem 1, Theorem 2, and Theorem 3 are robust in terms of Def. 4. For this purpose, we mainly use the triangle inequality and the following inequalities.

From $\langle \Psi | \mathcal{M} | \Psi \rangle > 1 - \epsilon$, it is $\|\Psi - \mathcal{M} | \Psi\rangle\| < \sqrt{2\epsilon}$, and it is $\|\Psi - \mathcal{M}_1 \mathcal{M}_2 | \Psi\rangle\| < \alpha + \beta$ for $\|\Psi - \mathcal{M}_1 | \Psi\rangle\|$, $\|\Psi - \mathcal{M}_2 | \Psi\rangle\|$ and if $\|\mathcal{M}_1\|_\infty = 1$.

We first bound the anti-commutation relations from Lemma 1 and Lemma 2 by counting the number of measurements involved in obtaining the anti-commutation relation on the first vertex, and then adding the number of times Lemma 2 has to be applied, which is the distance along the edges between the first vertex and any other vertex in the graph. The only exceptions are the vertices v_l, v_r in RE 3, where we use techniques from [50]. Consider Eq. (1) for the observables in the physical experiment \mathcal{I}_i simulating the I_i from Eqs. (B22)-(B25) for $i = 1, 2, 3, 4$. Explicitly, it is $|\sqrt{2}\langle \Psi | \mathcal{I}_1 | \Psi \rangle - (-1)^d| < \sqrt{2\epsilon}$, $|\sqrt{2}\langle \Psi | \mathcal{I}_2 | \Psi \rangle + (-1)^d| < \sqrt{2\epsilon}$ and $|\sqrt{2}\langle \Psi | \mathcal{I}_i | \Psi \rangle - 1| < \sqrt{2\epsilon}$ for $i = 3, 4$. It follows that $(-1)^d \sqrt{2}\langle \Psi | \mathcal{I}_1 | \Psi \rangle < -1 + \sqrt{2\epsilon}$, $(-1)^d \sqrt{2}\langle \Psi | \mathcal{I}_2 | \Psi \rangle > 1 - \sqrt{2\epsilon}$ and $\sqrt{2}\langle \Psi | \mathcal{I}_i | \Psi \rangle > 1 - \sqrt{2\epsilon}$ for $i = 3, 4$. As a result,

$$\langle \Psi | 4\mathbb{1} + \sqrt{2} ((-1)^d (\mathcal{I}_1 - \mathcal{I}_2) - \mathcal{I}_3 - \mathcal{I}_4) | \Psi \rangle < 4\sqrt{2}\epsilon.$$

Due to the operator's sums of squares decompositions, every squared element is equally bounded by

$$4\sqrt{2}\epsilon > \langle \Psi | \left[\frac{1}{2} ((-1)^d (\mathcal{I}_1 + \mathcal{I}_2) - \mathcal{I}_3 + \mathcal{I}_4) \right]^2 | \Psi \rangle = \left\| \left[\frac{1}{2} ((-1)^d (\mathcal{I}_1 + \mathcal{I}_2) - \mathcal{I}_3 + \mathcal{I}_4) \right] | \Psi \rangle \right\|_1^2.$$

It follows from Eq. C52 and Eq. C53 that

$$\begin{aligned} 4\sqrt{2}\epsilon &> \langle \Psi | \left[\mathcal{A}_0 - \frac{\mathcal{B}_0 - (-1)^d \mathcal{B}_1}{\sqrt{2}} \right]^2 | \Psi \rangle = \left\| \left[\mathcal{A}_0 - \frac{\mathcal{B}_0 - (-1)^d \mathcal{B}_1}{\sqrt{2}} \right] | \Psi \rangle \right\|_1^2, \\ 4\sqrt{2}\epsilon &> \langle \Psi | \left[\mathcal{A}_1 - \frac{\mathcal{B}_1 + (-1)^d \mathcal{B}_0}{\sqrt{2}} \right]^2 | \Psi \rangle = \left\| \left[\mathcal{A}_1 - \frac{\mathcal{B}_1 + (-1)^d \mathcal{B}_0}{\sqrt{2}} \right] | \Psi \rangle \right\|_1^2, \\ 4\sqrt{2}\epsilon &> \langle \Psi | \left[\frac{\mathcal{A}_0 - (-1)^d \mathcal{A}_1}{\sqrt{2}} - \mathcal{B}_0 \right]^2 | \Psi \rangle = \left\| \left[\frac{\mathcal{A}_0 - (-1)^d \mathcal{A}_1}{\sqrt{2}} - \mathcal{B}_0 \right] | \Psi \rangle \right\|_1^2, \\ 4\sqrt{2}\epsilon &> \langle \Psi | \left[\frac{\mathcal{A}_1 + (-1)^d \mathcal{A}_0}{\sqrt{2}} - \mathcal{B}_1 \right]^2 | \Psi \rangle = \left\| \left[\frac{\mathcal{A}_1 + (-1)^d \mathcal{A}_0}{\sqrt{2}} - \mathcal{B}_1 \right] | \Psi \rangle \right\|_1^2. \end{aligned}$$

To bound the anti-commutation relations $\left\| \left\{ \mathcal{O}_{v_l} \mathcal{R}_{d(v_l, v_r)}^{(O)}, \mathcal{Z}_{v_l} \mathcal{R}_{d(v_l, v_r)}^{(Z)} \right\} | \Psi \rangle \right\|_1$ and $\|\{\mathcal{X}_{v_r}, \mathcal{Z}_{v_r}\} | \Psi\rangle\|_1$, we use Eq. (C54) and Eq. (C55), respectively, together with the triangle inequality. As a result, it is

$$\left\| \left\{ \mathcal{O}_{v_l} \mathcal{R}_{d(v_l, v_r)}^{(O)}, \mathcal{Z}_{v_l} \mathcal{R}_{d(v_l, v_r)}^{(Z)} \right\} | \Psi \rangle \right\|_1 < \sqrt{8\sqrt{2}}(1 + \sqrt{2})\sqrt{\epsilon}, \quad (\text{F1})$$

$$\|\{\mathcal{X}_{v_r}, \mathcal{Z}_{v_r}\} | \Psi\rangle\|_1 < \sqrt{8\sqrt{2}}(1 + \sqrt{2})\sqrt{\epsilon}. \quad (\text{F2})$$

With the bound on the anti-commutation relations, we can bound the isometry using the triangle inequality whenever the anti-commutation relations or relations directly from the measurements are used with more details in [42]. Note that, when evaluating the isometry on the measurements applied to the state, we do not use additional anti-commutation relations; therefore, the bounds of Eq. (2) and Eq. (3) are the same. Then, a general bound is

$$\delta = \frac{\sqrt{\epsilon}}{2} \left((2|V| + |E|) (c + 4l) \right), \quad (\text{F3})$$

with the number of vertices $|V|$ and number of edges $|E|$ in the (inflated) graph. The parameter c_1 depends on the number of measurements needed to establish the first anti-commutation relation, and l is the largest distance along the edges from this vertex to any other. The parameter c_2 is the number of measurements involved in the mapping of $\mathcal{X}_u(\mathcal{Y}_u)$ to $\mathcal{Z}^{N(u)}$. For the different reference experiments, the parameters and bounds on δ are shown in Fig. I.

The bounds on δ are not optimal and can be improved, especially if more is known about the structure of the graph. Specifically, for larger graphs, it might be useful to combine several reference experiments when required subgraphs occur multiple times in the graph.